AEDC-TSR-78-V13
JUNE 1978
c.2

INFRARED AND PHASE-CHANGE PAINT MEASUREMENTS OF HEAT-TRANSFER ON THE SPACE SHUTTLE ORBITER

D. W. Stallings and D. B. Carver
ARO, Inc., AEDC Division
A Sverdrup Corporation Company
von Kármán Gas Dynamics Facility
Arnold Air Force Station, Tennessee

Period Covered: October 14, 1976 and
March 3-11, 1978

Approved for public release; distribution unlimited.

Reviewed By:

ERVIN P. JASKOLSKI, Captain, USAF
Test Director, VKF Division
Directorate of Test Operations

Approved for Publication:

FOR THE COMMANDER

CHAUNCEY D. SMITH, JR, Lt Colonel, USAF
Director of Test Operations
Deputy for Operations

Prepared for: NASA-JSC/ES3
Houston, TX 77058

ARNOLD ENGINEERING DEVELOPMENT CENTER
AIR FORCE SYSTEMS COMMAND
ARNOLD AIR FORCE STATION, TENNESSEE

REPORT DOCUMENTATION PAGE		READ INSTRUCTIONS BEFORE COMPLETING FORM
1. REPORT NUMBER AEDC-TSR-78-V13	2. GOVT ACCESSION NO.	3. RECIPIENT'S CATALOG NUMBER
4. TITLE *(and Subtitle)* Infrared and Phase-Change Paint Measurements of Heat Transfer on the Space Shuttle Orbiter		5. TYPE OF REPORT & PERIOD COVERED Final Report: October 4, 1976 & March 3-11, 1978 6. PERFORMING ORG. REPORT NUMBER
7. AUTHOR(s) D. W. Stallings and D. B. Carver, ARO, Inc., a Sverdrup Corporation Company		8. CONTRACT OR GRANT NUMBER(s)
9. PERFORMING ORGANIZATION NAME AND ADDRESS Arnold Engineering Development Center Air Force Systems Command Arnold Air Force Station, TN 37389		10. PROGRAM ELEMENT, PROJECT, TASK AREA & WORK UNIT NUMBERS Program Element 921E01
11. CONTROLLING OFFICE NAME AND ADDRESS Mrs. D. B. Lee NASA-JSC/EX3 Houston, Texas 77058		12. REPORT DATE July 1978 13. NUMBER OF PAGES 62
14. MONITORING AGENCY NAME & ADDRESS *(if different from Controlling Office)*		15. SECURITY CLASS. *(of this report)* UNCLASSIFIED 15a. DECLASSIFICATION/DOWNGRADING SCHEDULE N/A
16. DISTRIBUTION STATEMENT *(of this Report)* Approved for public release; distribution unlimited.		
17. DISTRIBUTION STATEMENT *(of the abstract entered in Block 20, if different from Report)*		
18. SUPPLEMENTARY NOTES Available in DDC.		
19. KEY WORDS *(Continue on reverse side if necessary and identify by block number)* space shuttle heat-transfer infrared		
20. ABSTRACT *(Continue on reverse side if necessary and identify by block number)* Heat transfer data were obtained on two Space Shuttle Orbiter models, one a 0.025-scale and the other a 0.04-scale. An infrared scanning camera and the phase-change paint technique were used to obtain data at Mach 8 for free-stream unit Reynolds numbers from 0.5×10^6 to 3.5×10^6 per foot. Gaps and steps in shuttle insulation material were simulated to determine the effect of such irregularities on the state of the boundary layer.		

DD FORM 1 JAN 73 1473 EDITION OF 1 NOV 65 IS OBSOLETE

CONTENTS

APPENDIXES

A. ILLUSTRATIONS

Figure

NOMENCLATURE

ALPHA-MODEL	Model angle of attack (not corrected for sting deflection), deg
ALPHA-MODEL-CORRECTED, α	Model angle of attack corrected for sting deflection, deg
ALPHA-SECTOR	Tunnel sector angle, deg
b	Model wing span, in.
BETA(TO), β, BETA (0.9TO)	Semi-infinite slab parameter $\beta = \frac{H(TAW)\sqrt{\Delta t}}{\sqrt{\rho c k}}$ for this test, data were also reduced with TAW defined as either TO or 0.9TO
c	Specific heat of model material, $\frac{Btu}{lbm-°R}$
C	Wing chord length, in.
CAMERA	Denotes location of camera recording paint pictures TOP - Camera on top of tunnel OS - Camera on operating side of tunnel
CONFIG	Model configuration code number
D	Groove depth, in.
DELTIME, Δt	Time model was exposed to flow before taking phase-change paint picture or IR digitizing, sec
GROUP	Identification number for each tunnel injection
H(TAW)	Model heat-transfer coefficient based on adiabatic wall temperature, $Btu/ft^2-sec-°R$
H(TO)	Model heat-transfer coefficient based on tunnel stilling chamber temperature, TO, $Btu/ft^2-sec-°R$
H(0.9TO)	Model heat-transfer coefficient based on 0.9TO, $Btu/ft^2-sec-°R$

HRFR — Reference heat-transfer coefficient based on Fay-Riddell theory, Btu/ft^2-sec-°R

$$= \left[\frac{8.172(PO1)^{0.5}(MU-0)^{0.4}(1-(P-INF)/PO1)^{0.25}}{(RN)^{0.5}\ (TO)^{0.15}}\right] \times \left[\overline{0.2235 + 0.0000135\ (TO + 560)}\right]$$

where PO1 - stagnation pressure downstream of a normal shock, psia

MU-0 = air viscosity based on TO, lbf-sec/ft^2

RN = reference nose radius for each model

RN_1 = 0.025 ft (94-0 Model)

RN_2 = 0.040 ft (82-1 and 82-3 Models)

INITIAL TEMP, T_I — Model temperature prior to a run, °R

INJECT TIME — Time required for model to reach centerline, sec

k — Model material thermal conductivity, Btu/ft-sec-°R

L — Model length, in.

MACH, M_∞ — Free-stream Mach number

MU-INF — Free-stream viscosity, lbf-sec/ft^2

PAINT TEMP — Denotes the rated melting temperature of the selected paint, °F

PCK1/2 — see $\sqrt{\rho ck}$

PIC NO — Denotes the frame number for each picture for a selected group. The number in brackets is the paint melt temperature in °F

P-INF, p_∞ — Free-stream pressure, psia

PO, P_o — Tunnel stilling chamber pressure, psia

RE/FT, Re_∞ — Free-stream unit Reynolds number, ft^{-1}

RHO-INF — Free-stream density, slugs/ft^3

ROLL NO — Identification number for each roll of paint film

S — Surface distance along groove, in.

TAW, T_{aw} — Adiabatic wall temperature, °R

For windward centerline of the 82-1 and 82-3 models a computed value was defined as

$TAW = TO\ [0.867 + 0.133\ (\sin(\alpha + \varepsilon))^{1.55}]$

	where ε = local model surface deflection angle, deg
TBAR (TO)	$\frac{TW - T_i}{TO - T_i}$, where TW is the measured model surface temperature
TBAR (0.9TO)	$\frac{TW - T_i}{0.9TO - T_i}$, where TW is the measured model surface temperature
T-INF, T_∞	Free-stream temperature, °R
T_{pc}	Phase change paint temperature, °F
TIME, t	Time, sec
TO, T_o	Tunnel stilling chamber temperature, °R
TW, T_w, TWALL	Measured model surface temperature, °R
V-INF	Free-stream velocity, ft/sec
W_b	Groove width at bottom of grove, in.
W_s	Groove width at about 0.025-in. below model surface, in.
x	Axial distance from nose of model, in.
X_A	Distance along section through grooves of forebody model, in. (see Fig. 18)
X_{CL}	Distance along windward centerline of forebody model, in. (see Fig. 18)
X_w	Distance from wing leading edge, in.
y	Spanwise distance from model centerline, in.
α	Model angle of attack, deg
ρ	Model material density, lbm/ft^3
$\sqrt{\rho ck}$	Square root of the product of the model density, specific heat and thermal conductivity, $Btu/ft^2\text{-}sec^{\frac{1}{2}}\text{-}sec°R$

1.0 INTRODUCTION

The work reported herein was conducted by the Arnold Engineering Development Center (AEDC), Air Force Systems Command (AFSC) at the request of the National Aeronautics and Space Administration Johnson Space Center (NASA-JSC), under Program Element 921E01, for Rockwell International Space Division. The NASA-JSC project monitor was Mrs. D. B. Lee and the RI project monitor was Mr. J. W. Cummings. The work was done by ARO, Inc., AEDC Division (a Sverdrup Corporation Company), contract operator of AEDC, AFSC, Arnold Air Force Station, Tennessee. The tests were conducted in the von Karman Gas Dynamics Facility (VKF) Hypersonic Wind Tunnel (B) on October 14, 1976 and March 3 through March 11, 1978 under ARO Project Numbers V41B-K7A (Rockwell designation MA-29), and V41B-P4A (Rockwell designation OH-90), respectively. Final data from this test were submitted to RI on April 7, 1978.

These tests were part of a large program to evaluate the effects of aerodynamic heating on the Space Shuttle Orbiter. The MA-29 test was a blockage study conducted to determine the maximum allowable model size for OH-90. The OH-90 test was specifically designed to study boundary layer transition on the lower surface of the orbiter wing. Gaps and steps in the wing insulation material were simulated to determine the effect of such irregularities on the state of the boundary layer. The final test shift of the OH-90 entry was done in support of the Rockwell OH-103 project. An orbiter forebody model was used to obtain detailed heat-transfer rate data on the forward 20 percent of the 140C Space Shuttle Orbiter configuration.

All tests were conducted in the 50-in. Hypersonic Wind Tunnel (B) at a free-stream Mach number of 8. The free-stream unit Reynolds number was varied from 0.5×10^6 to 3.5×10^6 per foot. Model angles-of-attack from 30 to 45-deg were run with zero model roll angle. Several model configurations with various insulation tile gaps and step heights were tested. An infrared scanning camera and the phase-change paint technique were used on different runs to measure the heat-transfer coefficient on the wing lower surface.

All test data, including detailed logs and other information required to use the data, have been transmitted to Rockwell International under separate cover as a Final Data Package. Inquiries to obtain copies of the test data should be directed to NASA-JSC/ES3, Houston, Texas 77058. One printed copy and a microfilm record were retained at AEDC in the VKF.

2.0 APPARATUS

2.1 TEST FACILITY

Tunnel B, Figure 1, is a closed-circuit hypersonic wind tunnel with a 50-in.-diam test section. Two axisymmetric contoured nozzles are available to provide Mach numbers of 6 and 8 and the tunnel may be operated continuously over a range of pressure levels from 20 to 300 psia at M_∞ = 6, and 50 to 900 psia at M_∞ = 8. Stagnation temperatures up to 1350°R are

obtained through the use of a natural gas-fired combustion heater. The entire tunnel (throat, nozzle, test section, and diffuser) is cooled by integral, external water jackets. The tunnel is equipped with a model injection system, which allows removal of the model from the test section while the tunnel remains in operation. A description of the tunnel may be found in Reference 1.

2.2 TEST ARTICLE

In order to maximize the model scale without blocking the wind tunnel, a partial model, with the right wing cut away, was planned for the OH-90 test. The blockage model, shown in Fig. 2, consisted of a flat plate cut to match the wing planform, with a cone-cylinder to simulate the fuselage.

Based on the results of the blockage tests, the OH-90 model, (referred to as the 94-0 model) shown in Fig. 3, was a 0.025-scale version of the Shuttle Orbiter. The basic model structure was steel, with interchangeable leading edge sections made of copper. Internal water passages were provided for cooling the leading edge. The wing lower surface panels, also interchangeable, were made of Novamide 700/55, an insulator with good radiation properties in the infrared region.

Details of the simulated insulation tiles are seen in Fig. 4. Two types of insulation, designated as reuseable surface insulator (RSI) and reinforced-carbon-carbon (RCC), will be used on the orbiter, and both were included in the design of the OH-90 model. The RSI simulation consisted of a single tile at each of six spanwise locations, as indicated in Fig. 4a. Two leading edge sections gave two different chordwise positions for these tiles (see Fig. 4a and 4b). Each individual tile could be adjusted to change the gap around the tile and the height of the tile above (or below) the wing surface. The RCC simulation consisted of copper and Novamide segments which could be rearranged as shown in Fig. 4c and 4d, with variable gaps between the segments. The model was fabricated by Rockwell and construction details are contained in Rockwell drawings SS-H-01851 through SS-H-01858.

Installation of the OH-90 model in Tunnel B is seen in Fig. 5. Installation of the MA-29 model was the same.

The forebody models were 0.04-scale models of the forward half of the Rockwell International Space Shuttle Orbiter 140C. Contours of the models are defined by Rockwell drawing VL70-000140C. Lockheed Missiles and Space Company (LMSC) of Huntsville, Alabama, subcontractors for model fabrication, cast the models from a proprietary epoxy material (Material LH), which has a low thermal diffusivity and relatively high strength. The models were cast as a one-piece shell with a nominal wall thickness of 1 in. and then filled with foam. Samples of the same batch of epoxy used to cast the models were analyzed by LMSC to determine the thermophysical properties (density, specific heat, and conductivity) which were necessary for data reduction. Photographs and details of the models and model components are shown in Figs. 6 through 8.

Two models were supplied for this test, both smooth. One of the models (82-1) was supplied with "paint stripes" to serve as reference coordinates (Fig. 7). These stripes were removed prior to the test. The other model (82-3) was modified, after arrival at AEDC, to simulate lateral grooves between tiles and a "missing tile" (Fig. 8). The basic model geometry is defined in Fig. 6 and a sketch of the model installation is shown in Fig. 9. Dimensions of the grooves which were added to the model are listed in Table 1.

2.3 TEST INSTRUMENTATION

Tunnel B stilling chamber pressure is measured with a 100- or 1000-psid transducer referenced to a near vacuum. Based on periodic comparisons with secondary standards, the accuracy (a bandwidth which includes 95-percent of residuals, i.e. 2σ deviation) of the transducers is estimated to be within ±0.1 percent of reading or ±0.06 psi whichever is greater for the 100-psid range and ±0.1 percent of reading or ±0.5 psi whichever is greater for the 1000 psid range. Stilling chamber temperature measurements are made with Chromel® Alumel® thermocouples which have an accuracy of ±(1.5°F + 0.375 percent of reading) based on repeat calibrations (2σ deviation).

The infrared system which was used to measure model surface temperatures on some runs utilizes an AGA Thermovision 680 camera which scans at the rate of 16 frames per second. The camera has a detector which is sensitive to infrared radiation in the 2 to 6 micron wavelength band. Infrared camera calibrations are performed with a standard black body reference source and have consistently been within ±1 percent of the camera manufacturer's calibration and are repeatable within ±1 percent in absolute temperature. A description of the VKF system is given in Reference 2.

Initial model temperatures were recorded for data reduction of the IR and phase-change paint data and the accuracy of the measurement is estimated to be ±1.0 percent. A total time differential for exposure to the tunnel flow is also required and the accuracy of this measurement is on the order of ±0.2 seconds. The interpretation of the wall temperature from the phase-change paint technique is estimated to be ±1.0 percent of the paint rated value.

3.0 TEST DESCRIPTION

3.1 TEST CONDITIONS

The tests were conducted in Tunnel B at a nominal Mach number of 8 over a free-stream unit Reynolds number range from 0.50 million to 3.5 million/ft. Data were taken at model angle-of-attack values of 30, 35, and 40 deg. The nominal tunnel test conditions are listed on the following page, while a complete test summary showing all configurations tested and the variables for each is presented in Table 2.

M_∞	P_o, psia	T_o, °R	p_∞, psia	Re_∞/ft x 10^{-6}
7.90	105	1260	0.012	0.50
7.92	155	1270	0.017	0.75
7.93	183	1275	0.020	0.88
7.94	210	1275	0.023	1.00
7.96	320	1290	0.034	1.50
7.97	342	1295	0.037	1.60
7.98	425	1300	0.044	2.00
7.99	555	1320	0.057	2.50
7.99	670	1330	0.070	3.00
8.00	800	1335	0.082	3.50

3.2 TEST PROCEDURES

3.2.1 General

In the VKF continuous flow wind tunnels (A, B, C), the model is mounted on a sting support mechanism in an installation tank directly underneath the tunnel test section. The tank is separated from the tunnel by a pair of fairing doors and a safety door. When closed, the fairing doors, except for a slot for the pitch sector, cover the opening to the tank and the safety door seals the tunnels from the tank area. After the model is prepared for a data run, the personnel access door to the installation tank is closed, the tank is vented to the tunnel flow, the safety and fairing doors are opened, and the model is injected into the airstream. After data acquisition is completed, the model is retracted into the tank and the sequence is reversed with the tank being vented to atmosphere to allow access to the model in preparation for the next run.

3.2.2 Phase-Change Paint Tests

After the completion of the camera installations and prior to the tests, photographs were taken of the 82-1 "paint stripe" model (see Fig. 7) at each of the model test attitudes. These photographs provided the model reference coordinates necessary for the data reduction. For the 94-0 model, the infrared reference grid, to be discussed in Section 3.3.2, served the same purpose.

The models were installed in an inverted position to facilitate photographic coverage of the windward surface (see Fig. 5 and 9). Prior to each run, the model was cleaned and cooled with alcohol and then spray painted with a phase-change paint (Tempilaq®). All painting was performed in the injection tank.

The paint temperature was chosen based on estimates of the expected heat-transfer coefficient and, as the test progressed, on the results from previous runs. The model initial temperature was measured and the model was injected into the tunnel flow for a test run. A television monitor was used to view the development of the melt patterns. The progress of the melt lines was photographed with 70-mm sequence cameras at the rate of one frame per second. When a satisfactory melt was observed

the model was retracted. Exposure time generally ranged from 10 to 30 seconds. After being retracted into the tank, the model was washed with alcohol to remove the remains of the old paint and also to cool it in preparation for the next run. A video tape system was used to provide an instant playback for monitoring purposes.

For the forebody models, two pairs of sequence cameras were used to record the photographs: two closeup cameras and two whole body cameras. The two closeup cameras were located on the top and operating side of the tunnel and were focused on the nose region of the model. The two whole body cameras were also located on the top and operating side of the tunnel, but their viewing area covered the entire model. Photographs were recorded using only one pair of cameras at a time. Closeup cameras were used to obtain detail data in the nose region, and the whole body cameras were used to obtain the heat-transfer distributions that might be affected by boundary-layer transition.

3.2.3 Infrared Tests

For infrared runs the desired model configuration was injected into the tunnel at the proper attitude, and the output of the IR camera was viewed on the color video monitor. The developing color patterns were observed as the model surface temperature increased. When the temperature was high enough to cause a satisfactorily strong signal from the camera, a single complete frame was digitized. The model was then retracted and cooled preparatory to the next run.

3.2.4 Data Acquisition

Instrumentation outputs were recorded using the VKF digital data scanner in conjunction with the VKF analog subsystem. All instruments other than the infrared camera were scanned at the rate of approximately ten times per second. Data acquisition began at model lift-off, under the control of a PDP 11/40 computer, utilizing the random access data system (RADS). The first data scan included all non-varying parameters, such as tunnel conditions and model attitude. For any time-dependent quantities the scan continued at the ten loop per second rate until the model left the tunnel centerline.

The AGA 680 infrared camera scanned the model to produce a complete picture at the rate of 16 frames per second. The camera output was recorded on analog tape and simultaneously displayed on a color television monitor. The increase in model surface temperature with time was thus observed, and a time was chosen to digitize a single frame of IR data. The model was exposed to the tunnel flow for between 10 and 30 seconds.

The phase-change paint melt patterns were recorded with cameras located on the top and side of the tunnel. Seventy-millimeter sequence photographs were taken at nominal one-second intervals, beginning at lift-off and continuing until the model left the tunnel centerline. While it was in the tunnel, the model was observed by means of a television camera. The video signal was recorded on tape for immediate playback and study prior to the next run.

Taken together, all the data obtained during a given injection cycle is termed a data group and is identified in the data tabulations by a group number.

3.3 DATA REDUCTION

For each group, the tabulated data begins with a listing of tunnel conditions and model information plus other pertinent parameters (e.g. IR camera f-stop or phase-change paint temperature) required to characterize the run and use the data. Following this the model heat-transfer data are presented.

Reduction of both infrared and phase-change paint data is based on the assumption that the surface temperature history is that of a homogeneous, semi-infinite slab (Ref. 3) subjected to an instantaneous and constant heat-transfer coefficient. The surface temperature rise is then given by:

$$\frac{T_w - T_i}{T_{aw} - T_i} = 1 - e^{\beta^2}(\text{erfc } \beta) \tag{1}$$

and

$$\beta = H(TAW)\sqrt{\Delta t}/\sqrt{\rho ck} \tag{2}$$

TAW was set equal to TO or 0.9TO, or, for the forebody models, calculated from

$$TAW = TO[0.867 + 0.133(\sin(\alpha + \varepsilon))^{1.55}] \tag{3}$$

The lumped thermophysical property, $\sqrt{\rho ck}$, was provided by Rockwell. It was a constant for the wing panel inserts of the 94-0 model and was a function of temperature for the 82-1 and 82-3 models. The values used are listed in Table 3.

The Fay-Riddell stagnation-point heat-transfer coefficient, HRFR (Ref. 4), based on a 0.025- or 0.04-ft-radius sphere, was used to normalize the computed aerodynamic heat-transfer coefficients. (The radius of this hypothetical sphere would be one foot for corresponding full-scale orbiter conditions).

3.3.1 Phase-Change Paint

For the paint data, the model surface temperature T_w in Equation 1 is set equal to the phase-change temperature of the paint being used for that particular data group. This then defines β. The only remaining quantity required to calculate the heat-transfer coefficient from Equation 2 is Δt, the time that the model has been exposed to the flow. This is recorded for each paint photograph. For a given photograph then, Eq. 2 defines a value of heat-transfer coefficient which corresponds to any observed boundary between melted and unmelted paint. Tracings of these boundaries are made from enlarged projections of the paint photographs from which it is a simple matter to make plots of heat-transfer coefficient versus distance by using the reference coordinates from the

"paint stripe" photographs. Selected photographs from the smooth forebody model are shown in Fig. 10 and the corresponding tracings are shown in Fig. 11.

During earlier paint tests (Ref. 5) using the forebody models, the model support sting was instrumented with strain gages to determine sting deflection. The results of the earlier work were curve-fit and entered in the present data reduction as an angle-of-attack correction.

3.3.2 Infrared

For the infrared data, the model surface temperature at any point is given by

$$T_w = \frac{K_2}{\ell n \left[1 + \frac{\gamma \varepsilon_o K_1}{(cnts - cntsr) + \frac{\gamma \varepsilon_r K_1}{\left(e^{K_2/T_r} - 1 \right)}} \right]} \tag{4}$$

where

T_w = temperature at point in question, °R

T_r = reference plate temperature, °R

ε_o = emissivity of model

ε_r = emissivity of reference plate

γ = IRTRAN window transmission factor

K_1, K_2 = constants defined for each IR camera lens and f-stop from calibration data using a black-body source

cnts = camera output at point in question, counts

cntsr = camera output at a point on the reference plate, counts

The temperature obtained from Equation 4 is used in Equation 1 to evaluate β. The heat-transfer coefficient is then calculated from Eq. 2, using an exposure time based on the time at which the IR frame was digitized.

One complete frame of infrared data consists of 70 scan lines with 110 points per line for a total of 7700 discrete spots. The above procedure is carried out to obtain a value of temperatuare and heat-transfer coefficient for each of these spots. Before these data are printed, the temperature is normalized by the initial (pre-injection) model surface temperature and the heat-transfer coefficient is normalized by the Fay-Riddell reference value.

The infrared data are presented in two other forms in addition to the digital data tabulations previously described. As discussed in Section 3.2.4, the output of the IR camera is displayed in real time on a color television monitor. A 70-mm camera was used to photograph the monitor screen simultaneously with the single frame digitizing process. On the television monitor the total temperature range which the system is set up tomeasure is divided, in a nonlinear fashion, into ten separate colors, starting with blue for the lowest temperature and progressing through white for the highest. Each color then represents a temperature band within the total range, and the interface between two colors corresponds to one particular temperature.

The color photographs of the infrared monitor can be used to obtain surface temperature if a calibration of color versus temperature is known. Such a calibration is a function of the sensitivity setting of the monitor, the camera f-stop, and the material emissivity. The emissivity of the Novamide 700/55 from which the lower surface wing panels were made was measured in the 2-6 micron band on a sample of the material supplied by RI. The camera spectral response is a function of wavelength, and when the spectral data from the Novamide were weighted with this factor, an effective emissivity of 0.96 was obtained. The temperatures at the nine color interfaces have been calculated for the f-stop/sensitivity combinations used in this test and are presented in Table 4. The f-stop, and sensitivity applicable to each group of data are given on the first page of the IR data printout.

The infrared data are also presented in the form of a contour map, as illustrated in Fig. 12. Figure 12a and 12b are grid line measurements explained below while Fig. 12c represents actual test data. The IR camera measures a count level for each of the 7700 spots in one frame. In the contour maps, each of 41 symbols is assigned a range of counts. The ranges do not overlap, so each of the 7700 spots is then represented by one symbol, and the computer prints the complete matrix of 7700 sumbols. The minimum count level used and the size of the increment represented by one symbol are variable, and by a judicious choice of these two parameters, it is usually possible to produce a map on which the background is suppressed so that the model stands out clearly, and contours of constant count level (and consequently constant heat-transfer coefficient) are readily discernible. This form of the data presentation is inherently qualitative. However, these maps are quite useful for locating "hot spots" and therefore are helpful in selecting the appropriate locations from which to plot the primary tabulated data.

In order for the IR data to be truly useful in making plots of heat-transfer coefficients versus model coordinates, it is necessary to define model positions in terms of Line and Point numbers. This was done by taking pre-test infrared pictures of the model with a grid-line pattern attached. The dimensions of the grid pattern are shown in Fig. 13. The pairs of numbers indicated at several of the intersections are the IR line and point numbers, respectively, which define the location of the intersection within the IR picture. With this information, and the accompanying model dimensions, any spot on the wing surface can be related to a spot in the IR picture. The contour maps shown in Figs. 12a and 12b correspond to the grid patterns of Figs. 13a and 13b respectively.

4.0 UNCERTAINTY OF MEASUREMENTS

An evaluation of the influence of random measurement errors is presented in this section to provide a partial measure of the uncertainty of the final test results presented in this report. Although evaluation of the systematic measurement error (bias) is not included, it should be noted that the instrumentation accuracy values (given in Section 2.3) used in this evaluation represent a combination of both systematic and two-sigma random error contributions.

4.1 TEST CONDITIONS

Accuracy of the basic tunnel parameters P_o and T_o (see Section 2.3) and the two-sigma deviation in Mach number determined from test section flow calibrations were used to estimate uncertainties in the other free-stream properties, using the Taylor series method of error propagation, i.e.

$$(\Delta F)^2 = \left(\frac{\partial F}{\partial X_1}\Delta X_1\right)^2 + \left(\frac{\partial F}{\partial X_2}\Delta X_2\right)^2 + \left(\frac{\partial F}{\partial X_3}\Delta X_3\right)^2 \ldots + \left(\frac{\partial F}{\partial X_n}\Delta X_n\right)^2 \qquad (5)$$

where ΔF is the absolute uncertainty in the dependent parameter $F = f(X_1, X_2, X_3 \ldots X_n)$; $X_1, X_2, X_3 \ldots X_n$ are the independent measurements; and $\Delta X_1, \Delta X_2, \Delta X_3 \ldots \Delta X_n$ are the errors in the independent measurements.

		Uncertainty (±), percent				
M_∞	RE/FT x 10^{-6}	M_∞	P_o	T_o	HRFR	RE/FT
7.90	0.50	0.4	0.48	0.4	1.0	1.2
7.92	0.75	↓	0.32	↓	↓	↓
7.93	0.88	↓	0.27	↓	↓	↓
7.94	1.00	↓	0.24	↓	↓	↓
7.96	1.50	0.3	0.16	↓	0.8	1.0
7.97	1.60	↓	0.15	↓	↓	↓
7.98	2.00	↓	0.12	↓	↓	↓
7.99	2.50	↓	0.10	↓	↓	↓
7.99	3.00	↓	↓	↓	↓	↓
8.00	3.50	↓	↓	↓	↓	↓

The uncertainty in model angle of attack (α) is estimated to be ±0.5 deg.

4.2 TEST DATA

In this test, data were obtained using the AGA 680 Thermovision System and temperature sensitive phase-change paint. The influence of random measurement errors for each of these techniques is presented in this section.

Heat-transfer coefficient measurements, H(0.9TO), for the IR runs ranged from about 0.02 to 0.002 Btu/ft^2-sec-°R. Overall estimated uncertainty in absolute values of heat-transfer coefficient for this measurement technique are as follows:

H(0.9TO), Btu/ft^2-sec-°R	Uncertainty (±), percent
~0.002	15
~0.020	12

An accurate estimate of the precision of phase-change paint data is hampered by the fact that an observer must determine the location of the melt line (Ref. 6). For the results presented in this report, only uncertainties attributable to the measured parameters are considered. The estimated uncertainty in H(0.9TO) for the paint technique is:

T_{pc}	Uncertainty (±), percent
< 660 °R (200°F)	14
> 660 °R (200°F)	11

These values were derived using the previously discussed Taylor series method of error propagation with the instrumentation accuracies listed in Section 2.3, combined with the accuracies below:

Item	Estimated Accuracy (±)
$\sqrt{\rho ck}$	±10% of measured value
T_i	±1.0% of measured value
$TW)_{IR}$	±1.2% of measured value
$TW)_{phase-change}$	±1.0% of paint rated value
TAW	±0.4%
$\Delta t)_{IR}$	±0.1 sec absolute
$\Delta t)_{phase-change}$	±0.2 seconds absolute

The uncertainties in heat-transfer coefficient are applicable for Δt greater than 5 sec, provided that the semi-infinite solid assumption is not violated. Certain regions of the model may not behave exactly as a semi-infinite solid (e.g. near sharp corners and in regions of extra large thermal gradients), and special considerations are required to define the data uncertainty in these regions. It should be noted that the dominant term in the uncertainty calculations for IR and phase-change paint technique is the accuracy of the model thermal properties (ρck).

5.0 DATA PACKAGE PRESENTATION

Data from the blockage test consisted of go - no go determinations based mainly on observations of the shock waves on the model by means of the shadowgraph system. The shadowgraph pictures have previously been

delivered to RI. Included in this report is a summary of the tunnel conditions and model attitudes tested and the results for each. This is presented in Table 5. Based on the results of the blockage study, a 0.025-scale model was chosen for the OH-90 test.

Digital data obtained from the IR system on the OH-90 model were plotted along the chord of the wing for spanwise locations corresponding to the tile positions. A sample of such a plot is shown in Figure 14. The data are for a smooth wing (tile height = gap = 0.0) and are from IR line number 51, which corresponds to y/b/2 = 0.9, the most outboard tile location. Using the gridline tare information the data can be scaled to match IR points with distance along the chord. This has been done in Figure 15. Note that the curve is reversed from left to right, since IR point number decreases from leading edge to trailing edge of the wing. For comparison, data are shown from the OH-56 test. These data were obtained on a 0.08-scale model of the outboard 28 percent of the orbiter wing tip. Assuming geometric similarity, the data may be adjusted for model scale effects and Reynolds number mismatch using the following equation, which may be deduced from the results of Reference 7.

$$\left(\frac{H(0.9TO)}{HRFR}\right)_1 = \left(\frac{Re_{\infty 1}}{Re_{\infty 2}}\right)^{0.3} \times \left(\frac{RN_1}{RN_2}\right)^{0.3} \times \left(\frac{H(0.9TO)}{HRFR}\right)_2 \qquad (6)$$

Using this equation to adjust the OH-90 IR data to match the conditions of the OH-56 test gives the results shown by the closed symbols in Fig. 15. Agreement between the data from the two tests is then seen to be reasonable.

For the 0.04-scale forebody models, representative windward centerline heat-transfer distributions at α = 30 deg are compared to previous data (References 5, 8, and 9) in Figure 16. The data agreement is very good and considered adequate for validation of the basic test results. H(TAW) was used for this comparison to minimize correlation errors resulting from wall temperature mismatch between the different test techniques included in Figure 16. Adjustment using Equation 6 was not necessary since model scale was the same for all the data of Figure 16.

The importance of using the proper adiabatic wall temperature is illustrated in Fig. 17, where the same data are compared using 0.9TO as the adiabatic wall temperature (Fig. 17b), as well as TAW (Fig. 17a). Comparison of Figs. 17a and b shows the H(TAW) data agreement to be significantly better than the H(0.9TO) data agreement. Near the stagnation point, the difference is dramatic with the paint data being as much as 50 percent higher than the thin-skin data where H(0.9TO) is used. These differences are a result of the wall temperature difference at which the two types of data were obtained. The wall temperatures for the paint data are the paint temperatures (T_{pg}), and the thin-skin data wall temperatures were typically less than 140°F yielding a value of T_w/T_o near 0.5. The paint data were obtained in the range $0.55 \lesssim T_w/T_o \lesssim 0.78$. This effect was not observed in the data of Fig. 15, since TAW on the wing lower surface is approximately equal to $0.9T_o$.

Typical data tabulations are shown in Figure 18. A group of phase-change paint data for the forebody model is presented in Figure 18a. Tabulations for the 94-0 orbiter model were similar. They include various tunnel and model information pertinent to the particular data group, and tabulations of heat-transfer coefficients corresponding to the time that each paint photograph was taken.

In Figure 18b, page numbers 1, 2, and 14 from a total of 25 pages are presented for a typical infrared data group. Again the pertinent tunnel and model information are listed. These are followed by the non-dimensional wall temperature and heat-transfer coefficient calculated for each of the 7700 spots in the complete IR frame.

A complete set of data tabulations, plots, and melt line tracings were included in the Final Data Package for this project.

REFERENCES

1. Sivells, James C. "Aerodynamic Design and Calibration of the VKF 50-In. Hypersonic Wind Tunnels," AEDC-TDR-62-230 (AD299774), March 1963.

2. Boylan, D. E., Carver, D. B., Stallings, D. W. and Trimmer, L. L. "Measurement and Mapping of Aerodynamic Heating Using a Remote Infrared Scanning Camera in Continuous Flow Wind Tunnels," AIAA Paper 78-799, April 1978.

3. Jones, Robert A. and Hunt, James L. "Use of Fusible Temperature Indicators for Obtaining Quantitative Aerodynamic Heat-Transfer Data," NASA-TR-R-230, February 1966.

4. Fay. J. A. and Riddell, F. R. "Theory of Stagnation Point Heat Transfer in Dissociated Air," Journal of the Aerospace Sciences, Vol. 25, No. 2, pp. 73-85, 121, February 1958.

5. Carver, D. B. "Heat-Transfer Tests on the Rockwell International Space Shuttle Orbiter with Boundary-Layer Trips," AEDC-TR-76-28, May 1976.

6. Matthews, R. K. and Gilley, G. E. "Reduction of Photographic Heat-Transfer Rate Data at AEDC," AEDC-TR-73-90 (AD762928), June 1973.

7. Widhopf, G. F. "Heat Transfer Correlations for Blunt Cones at Angle of Attack," SAMSO-TR-71-157, July 1971.

8. Hube, F. K. "Standard Thermal Protection Tile Roughness Effects on Windward Surface Heat Transfer on the Rockwell International Space Shuttle Orbiter," AEDC-TR-76-98, January 1977.

9. Knox, E. C., "Heat Transfer Test on the NASA/Rockwell International Space Shuttle Orbiter at Mach Number 8.0 in AEDC/VKF Tunnel B," AEDC-TSR-78-V10, June 1978.

APPENDIX

ILLUSTRATIONS

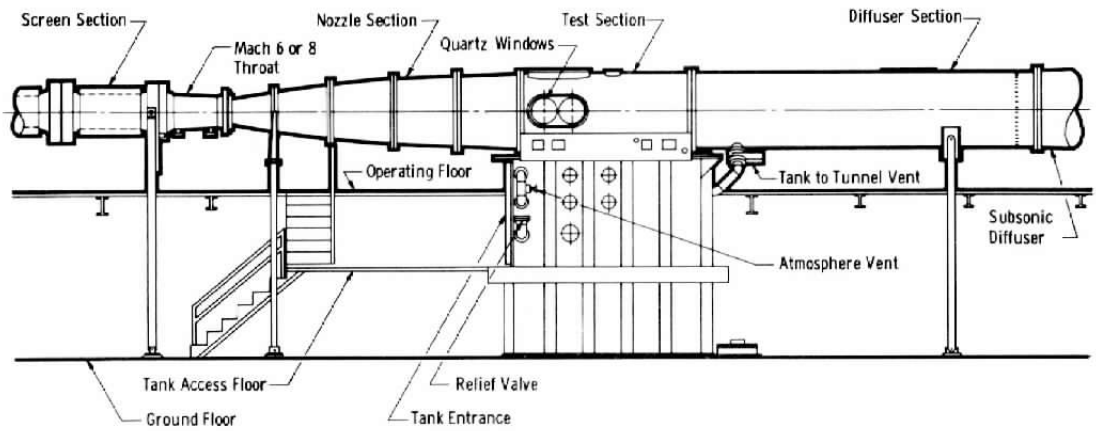

a. Tunnel assembly

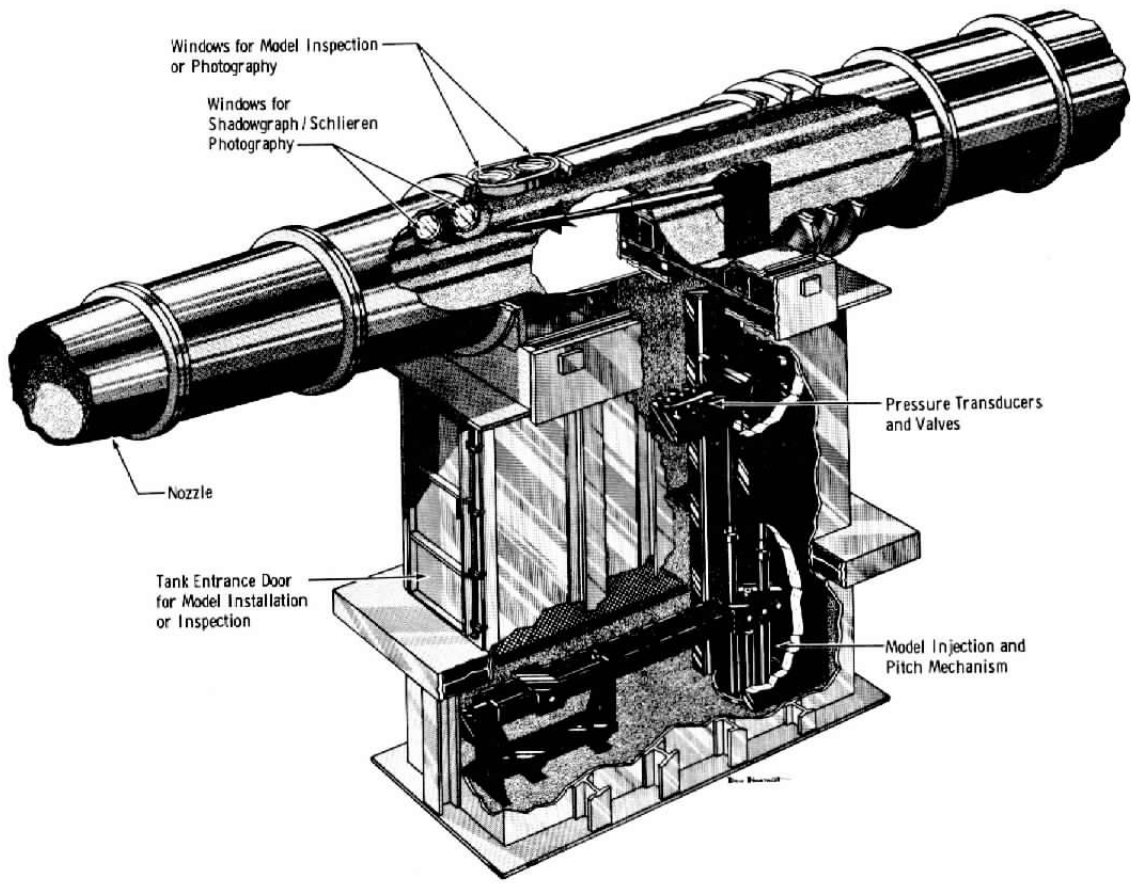

b. Tunnel test section

Fig. 1. Tunnel B

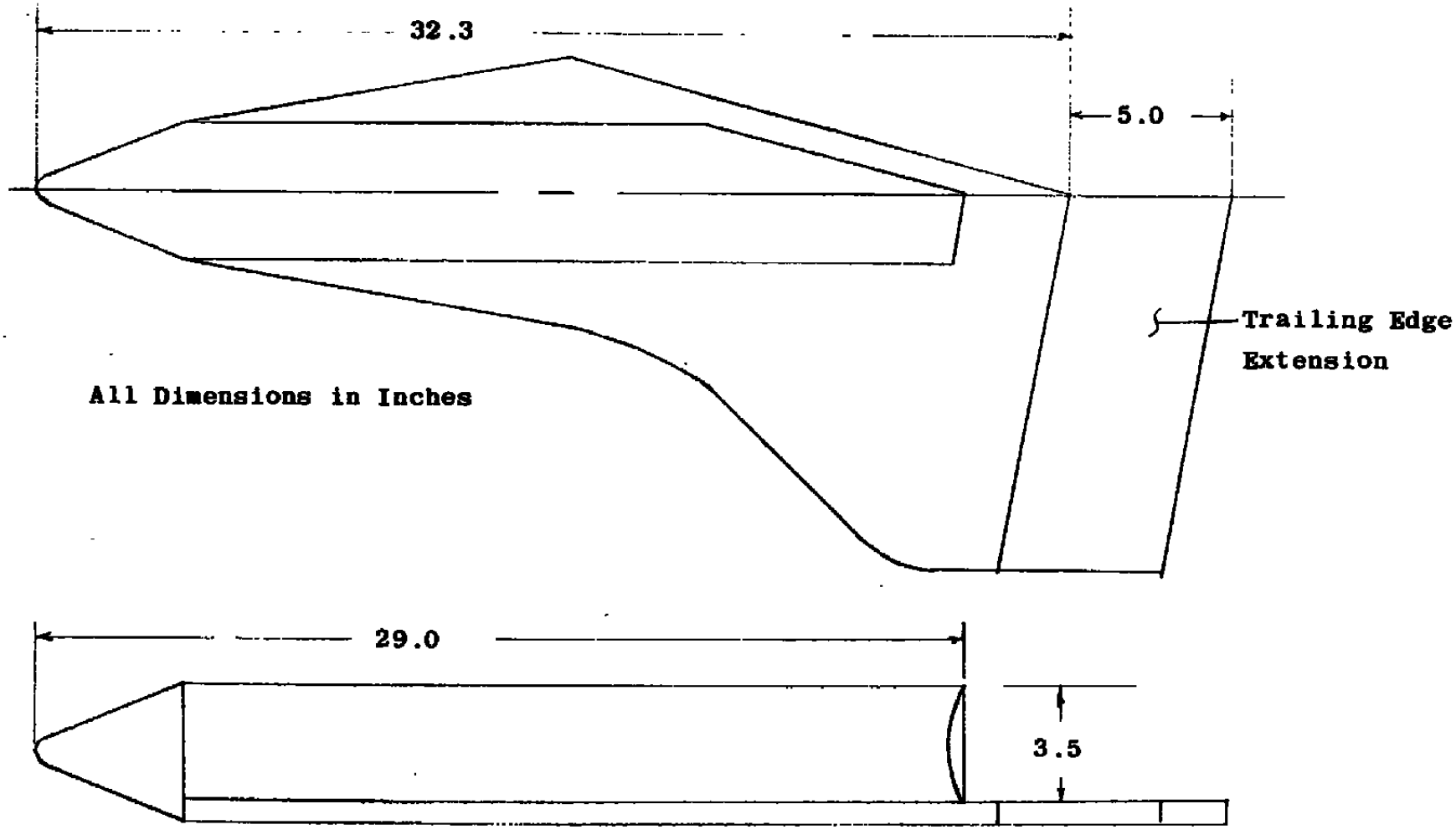

Figure 2 MA-29 Blockage Model

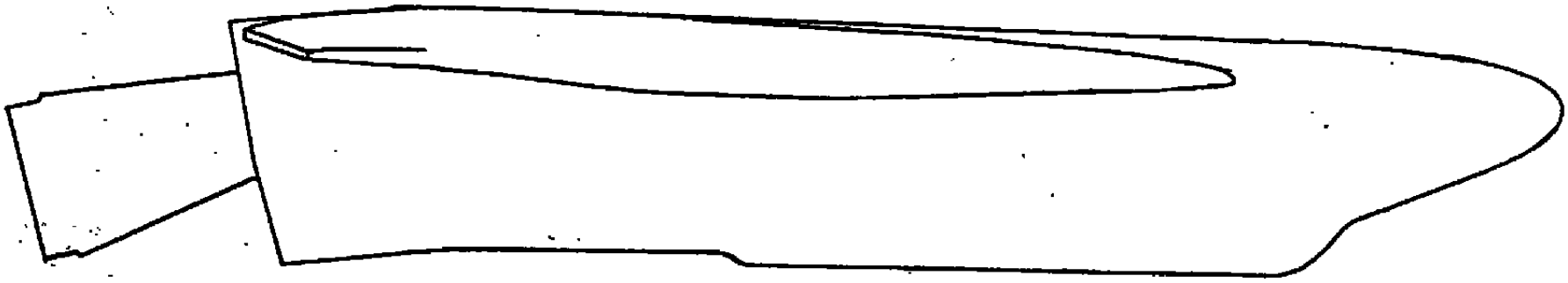

All Dimensions in Inches

Right Side Elevation

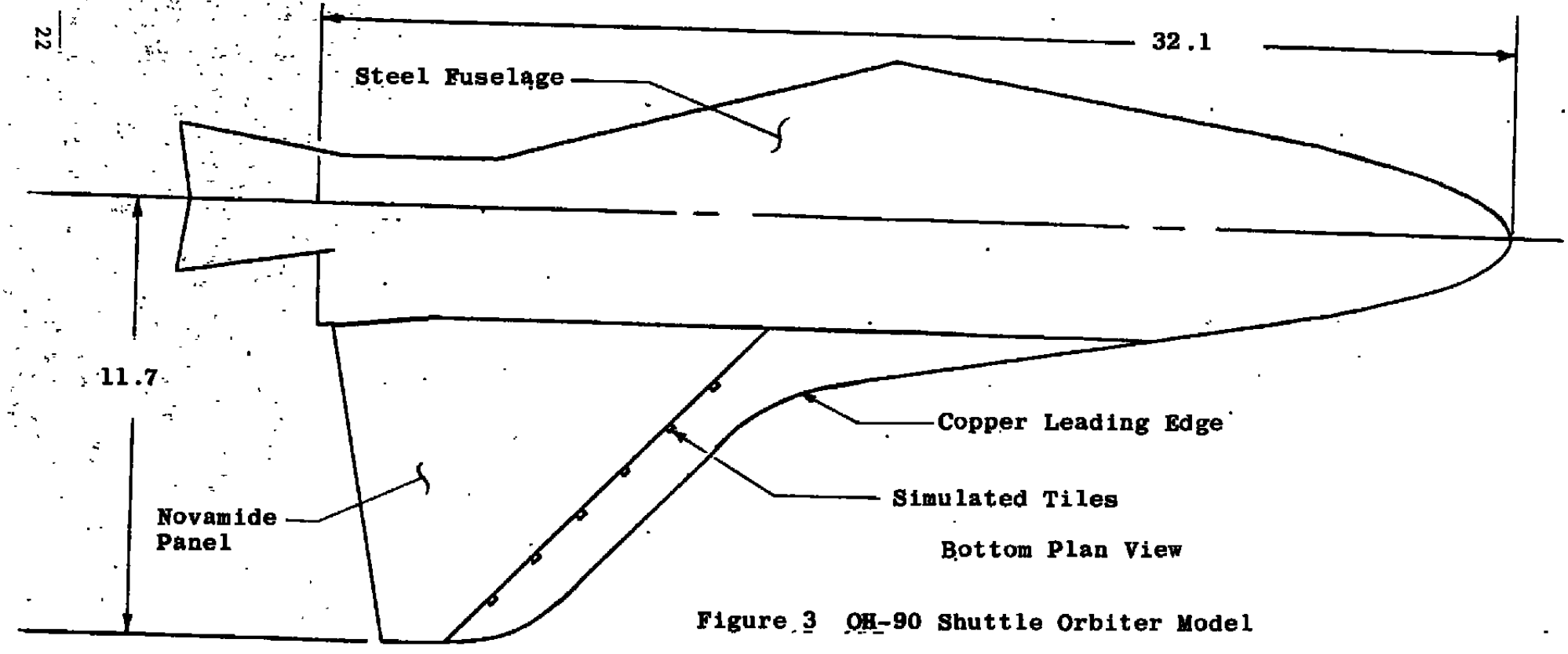

Figure 3 OH-90 Shuttle Orbiter Model

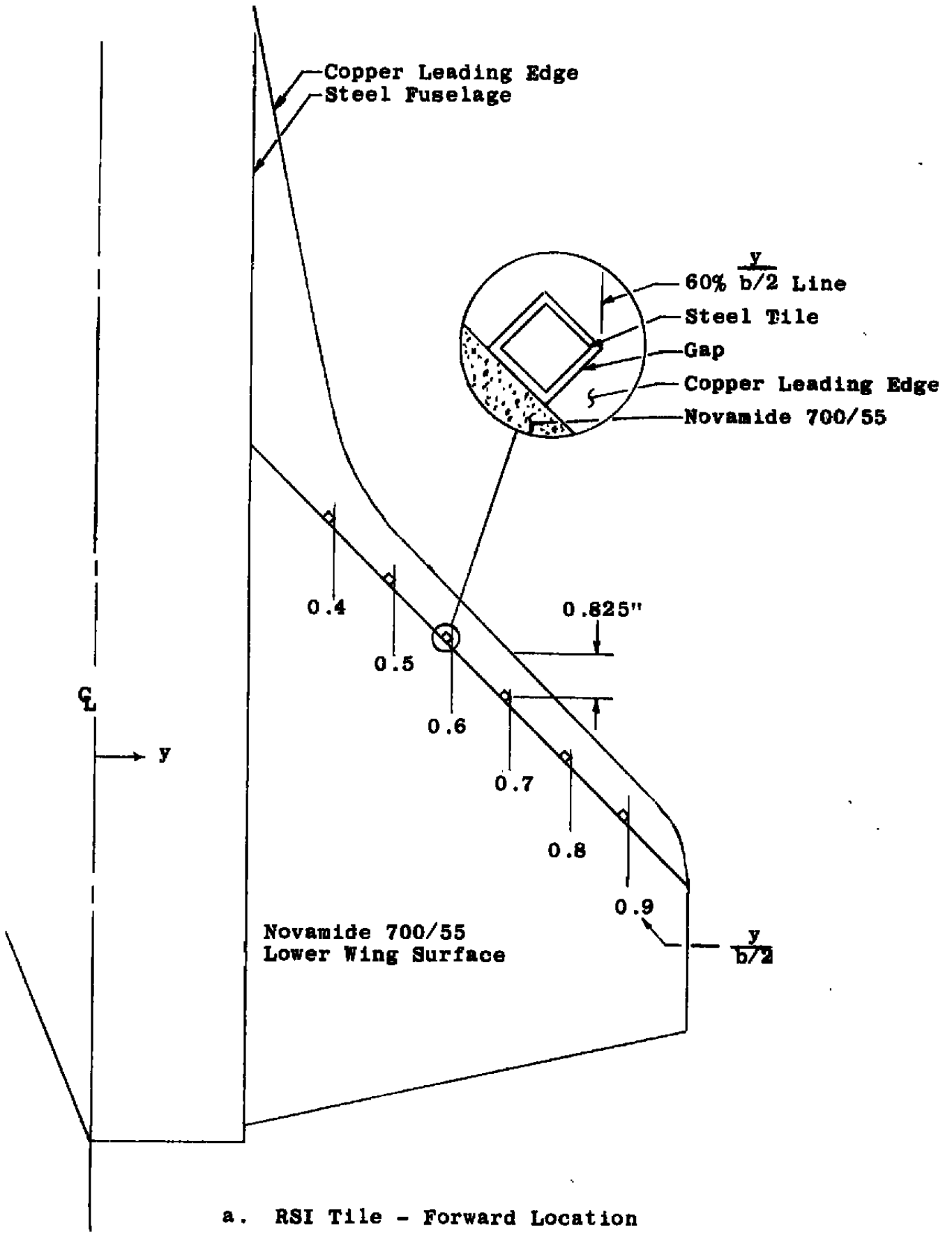

a. RSI Tile - Forward Location

Figure 4 Tile Simulation Details

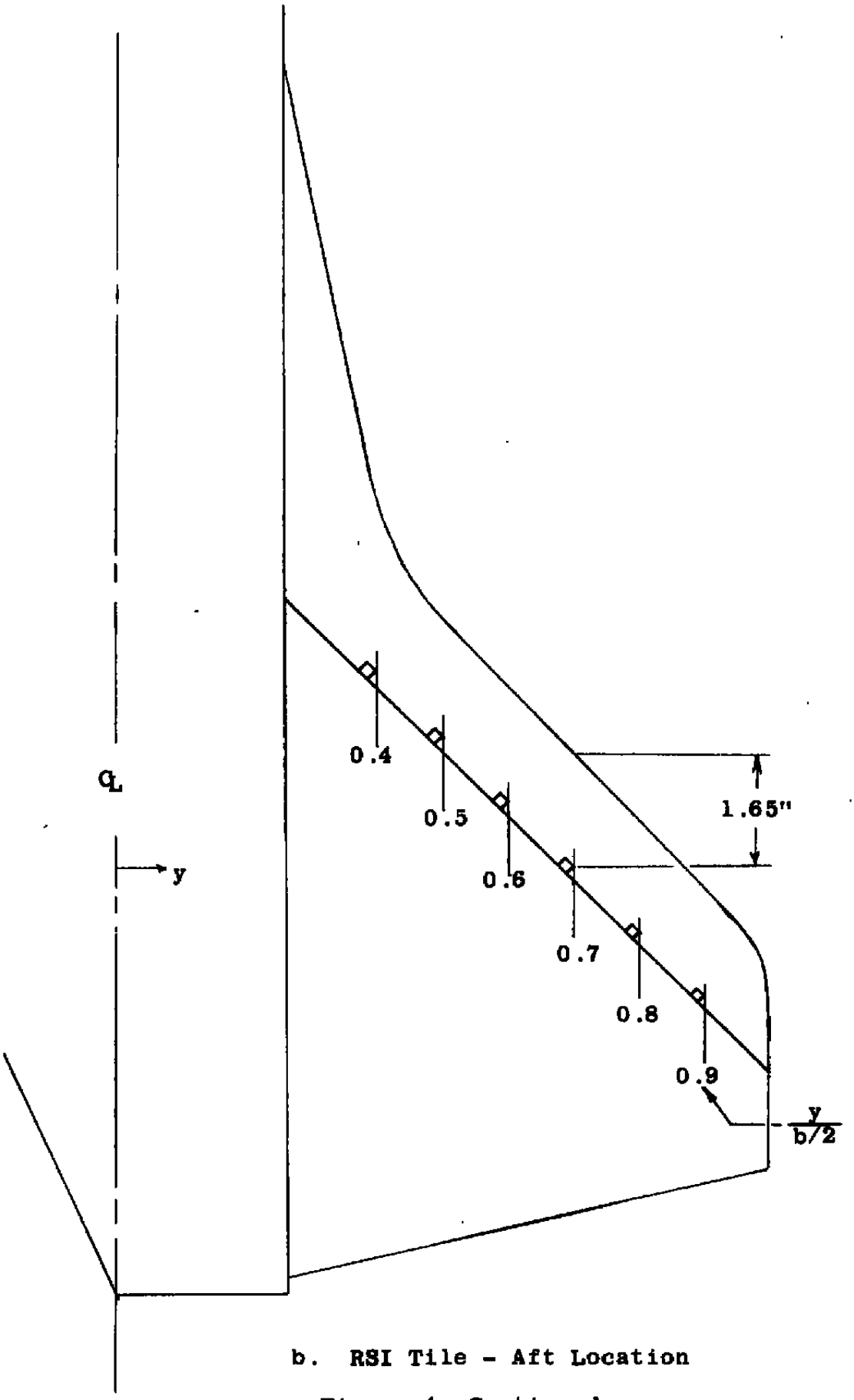

b. RSI Tile - Aft Location

Figure 4 Continued

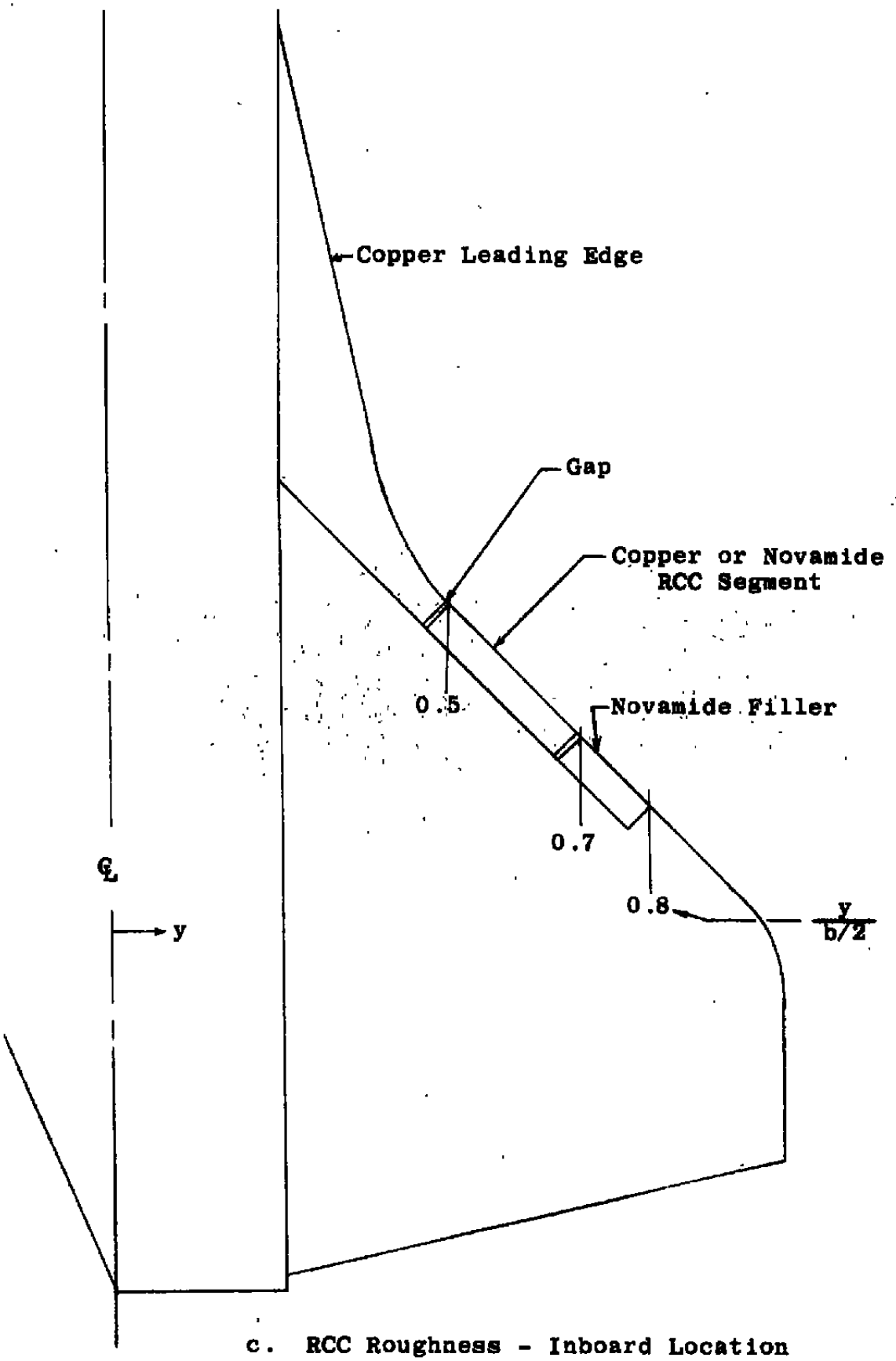

c. RCC Roughness - Inboard Location

Figure 4 Continued

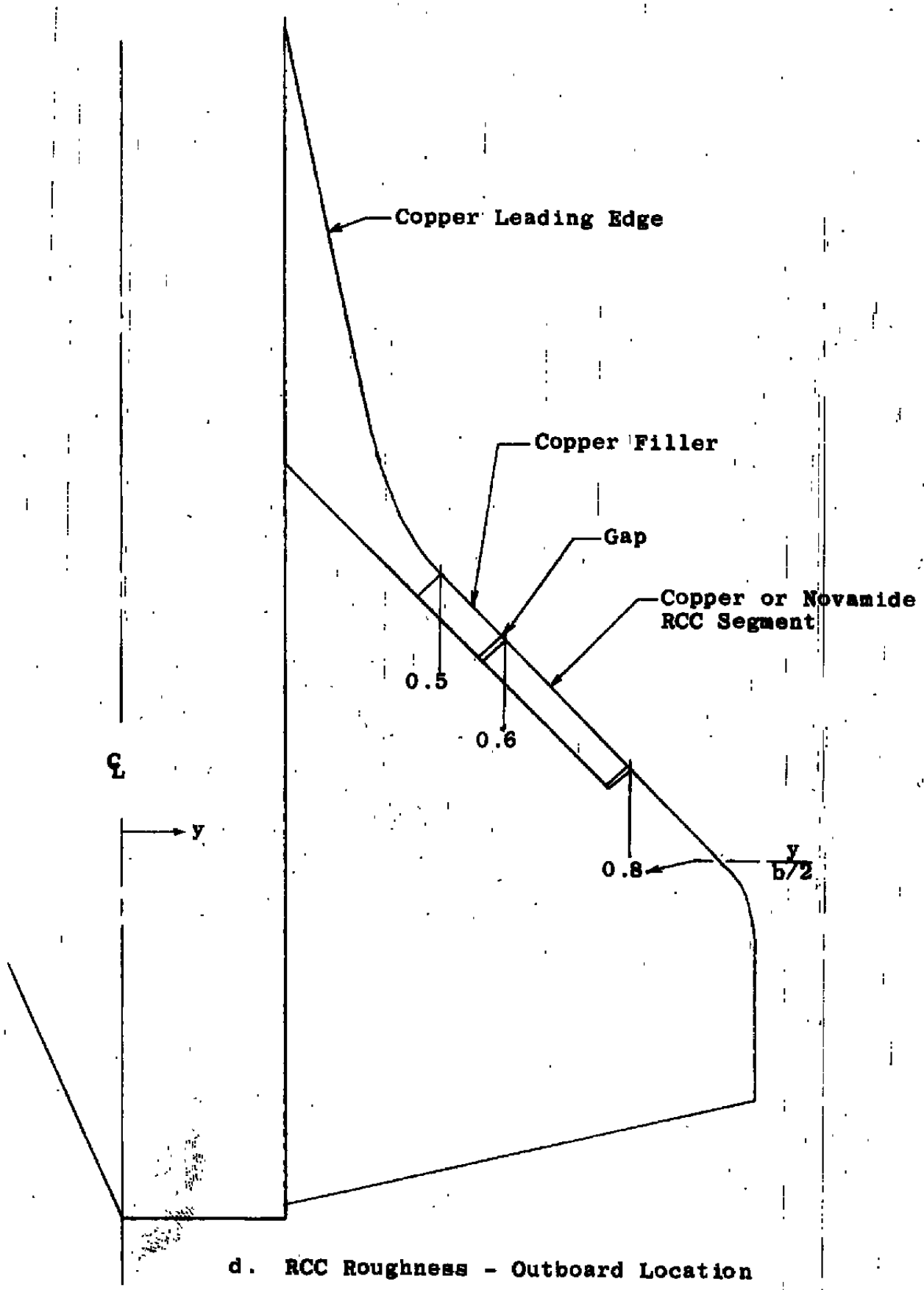

d. RCC Roughness - Outboard Location

Figure 4 Concluded

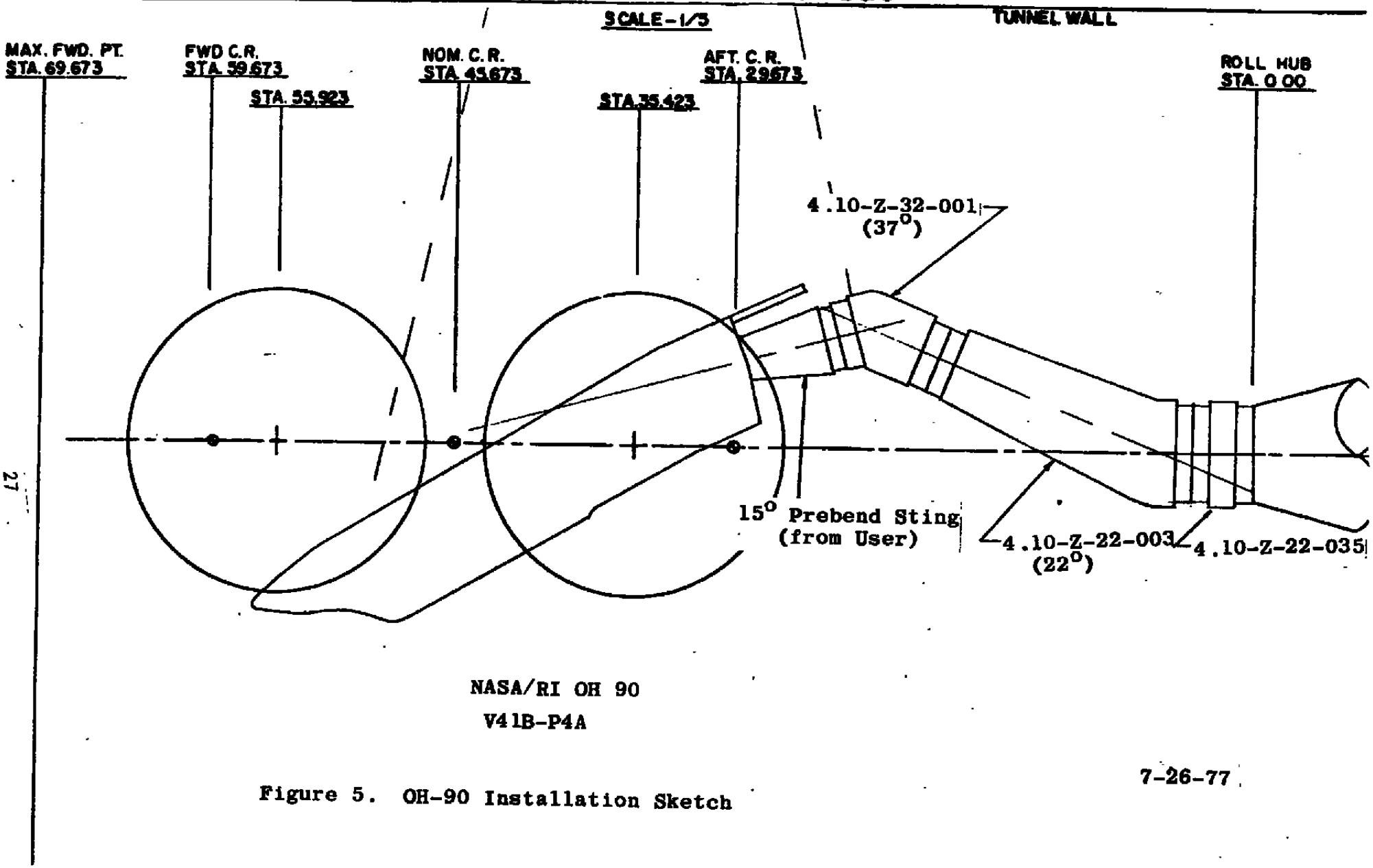

NASA/RI OH 90

V41B-P4A

7-26-77

Figure 5. OH-90 Installation Sketch

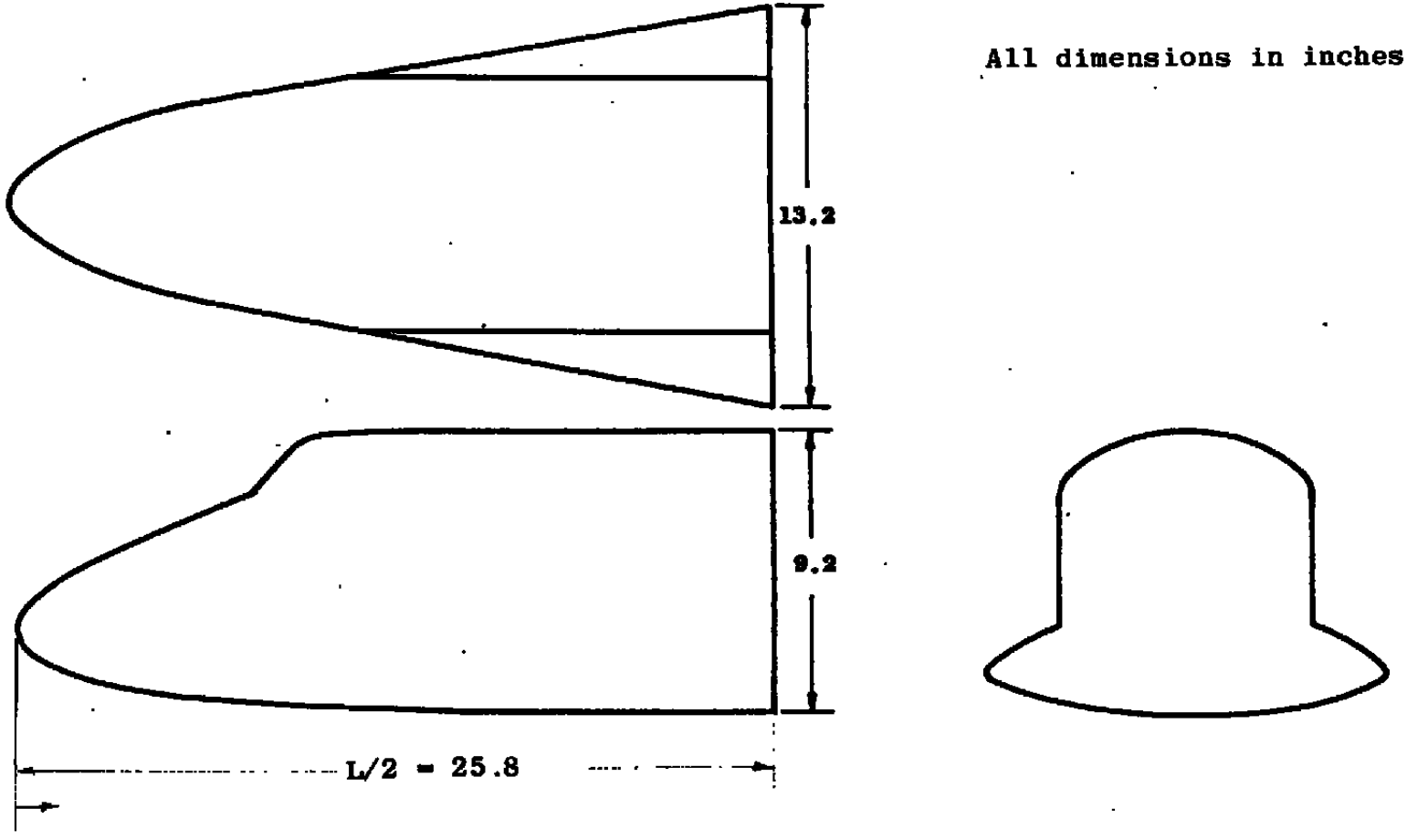

Figure 6. Sketch of Orbiter Forebody Models

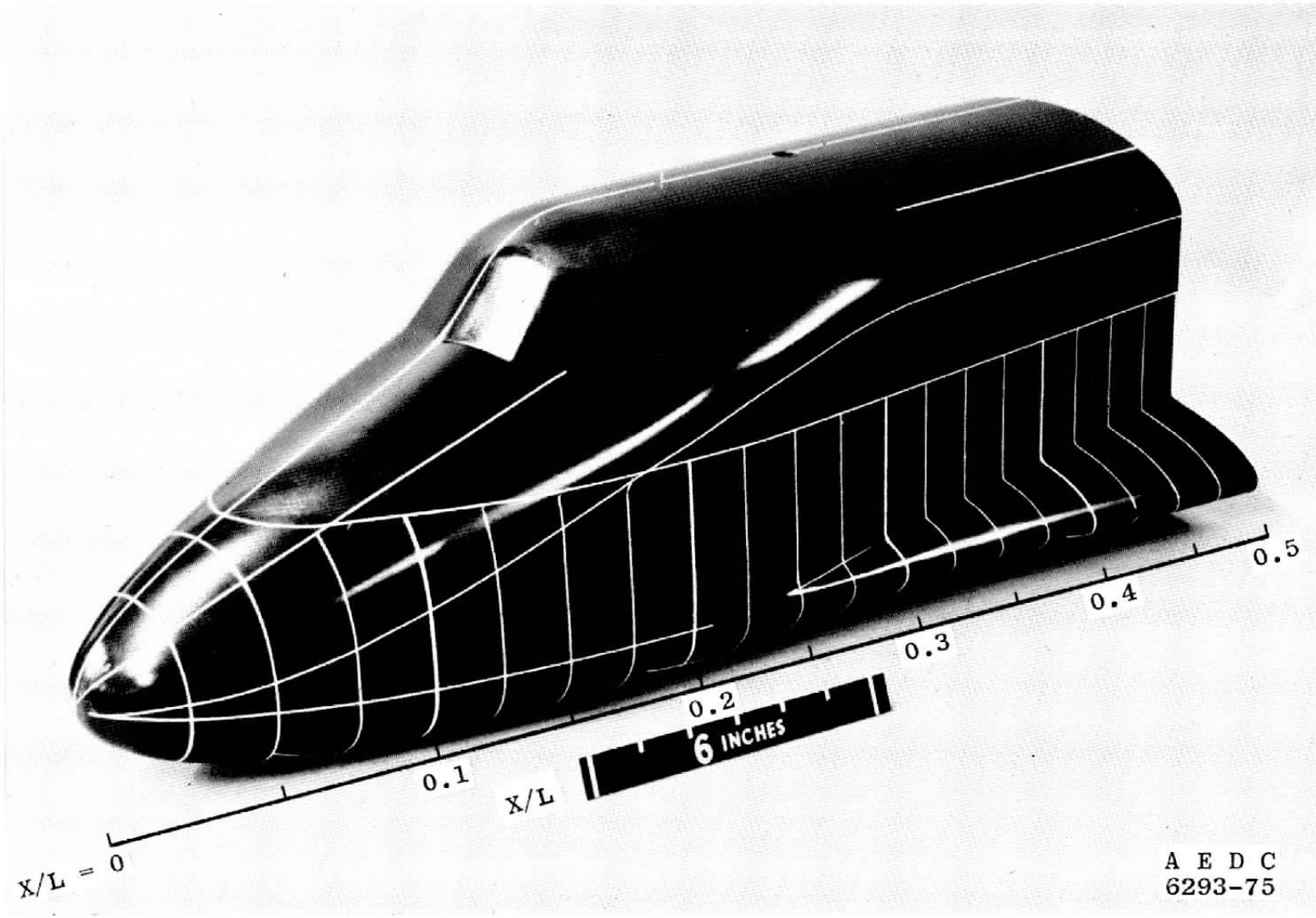

a. Photograph

Figure 7. Paint Stripe Model

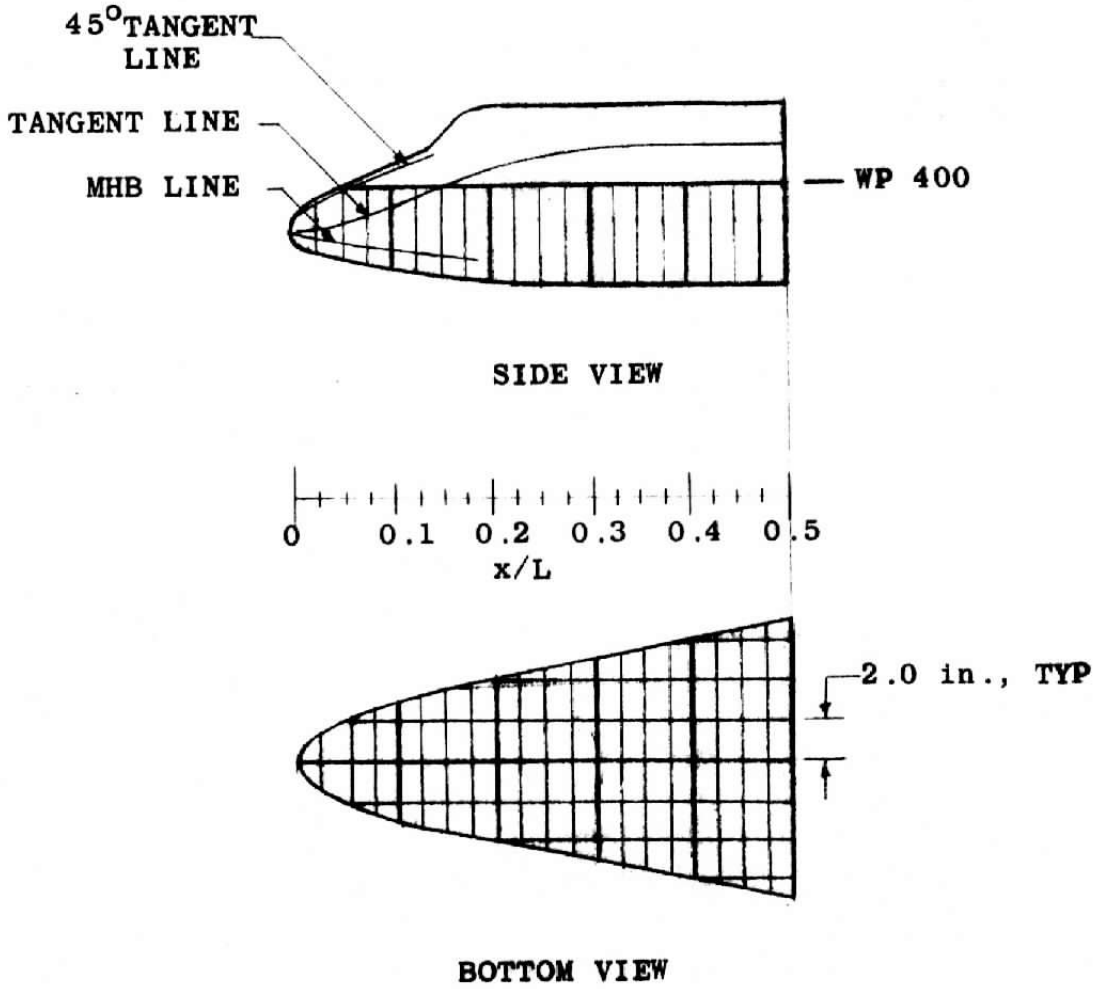

b. Stripe Locations

Figure 7. Concluded

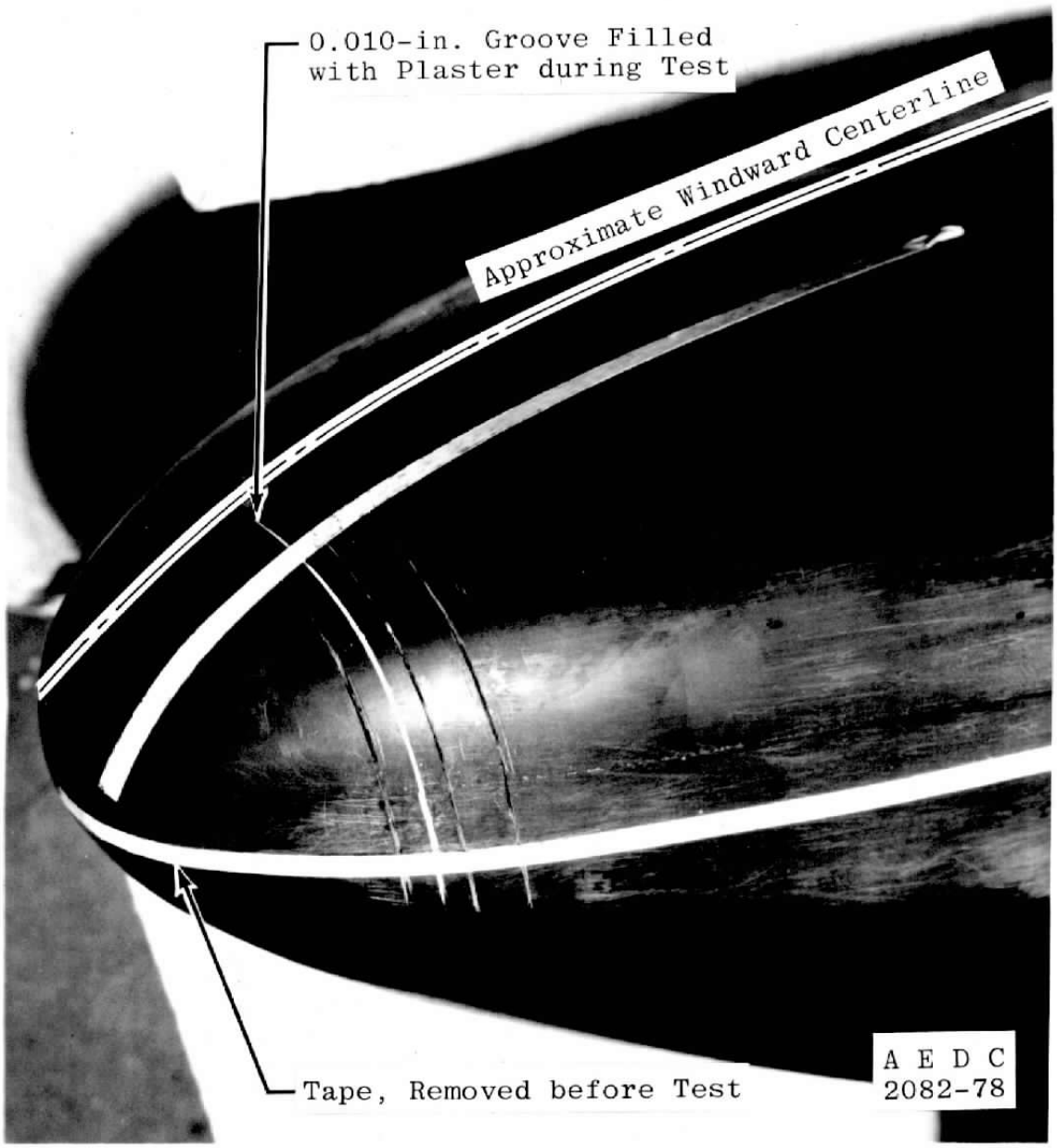

a. Photograph of ≈0.010-in. Grooves

Figure 8. Details of the Grooves and Missing Tile

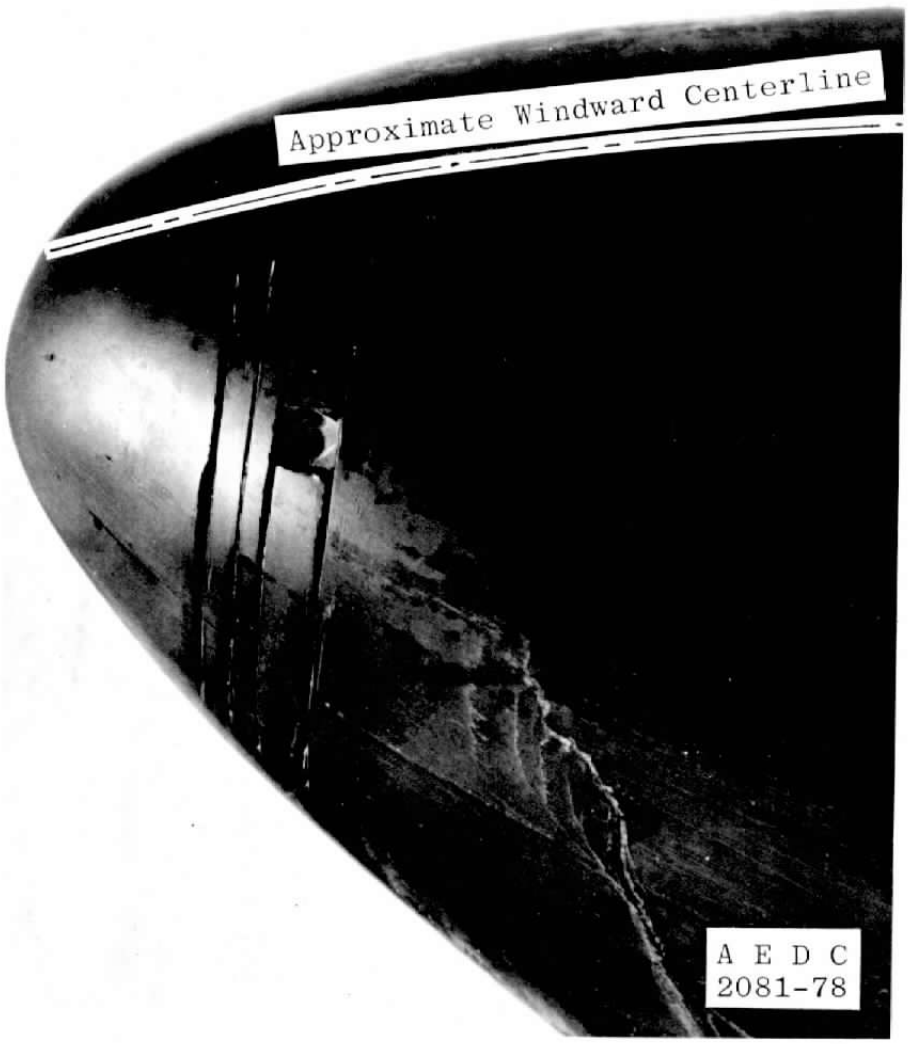

b. Photograph of ≈0.030-in. Grooves and Missing Tile
Figure 8. Continued

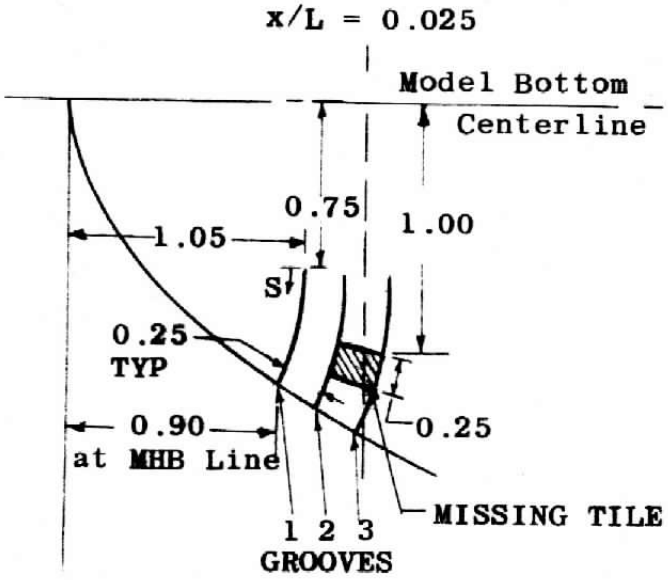

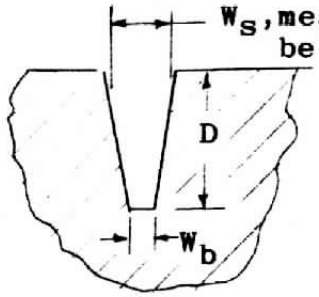

ENLARGED CROSS-SECTION OF GROOVE

Notes:
1. All dimensions in inches
2. Grooves were cut using jeweler's saw to obtain a nominal groove width of 0.010-in. (CONFIG 2)
3. Grooves were widened using a small hacksaw to obtain a nominal groove width of 0.03-in. (CONFIG 3)
4. Missing tile was simulated by drilling with 0.25-in. diam drill and cutting corners out with a knife.
5. See Table 1 for groove measurements.

c. Location of Grooves and Missing Tile

Figure 8. Concluded

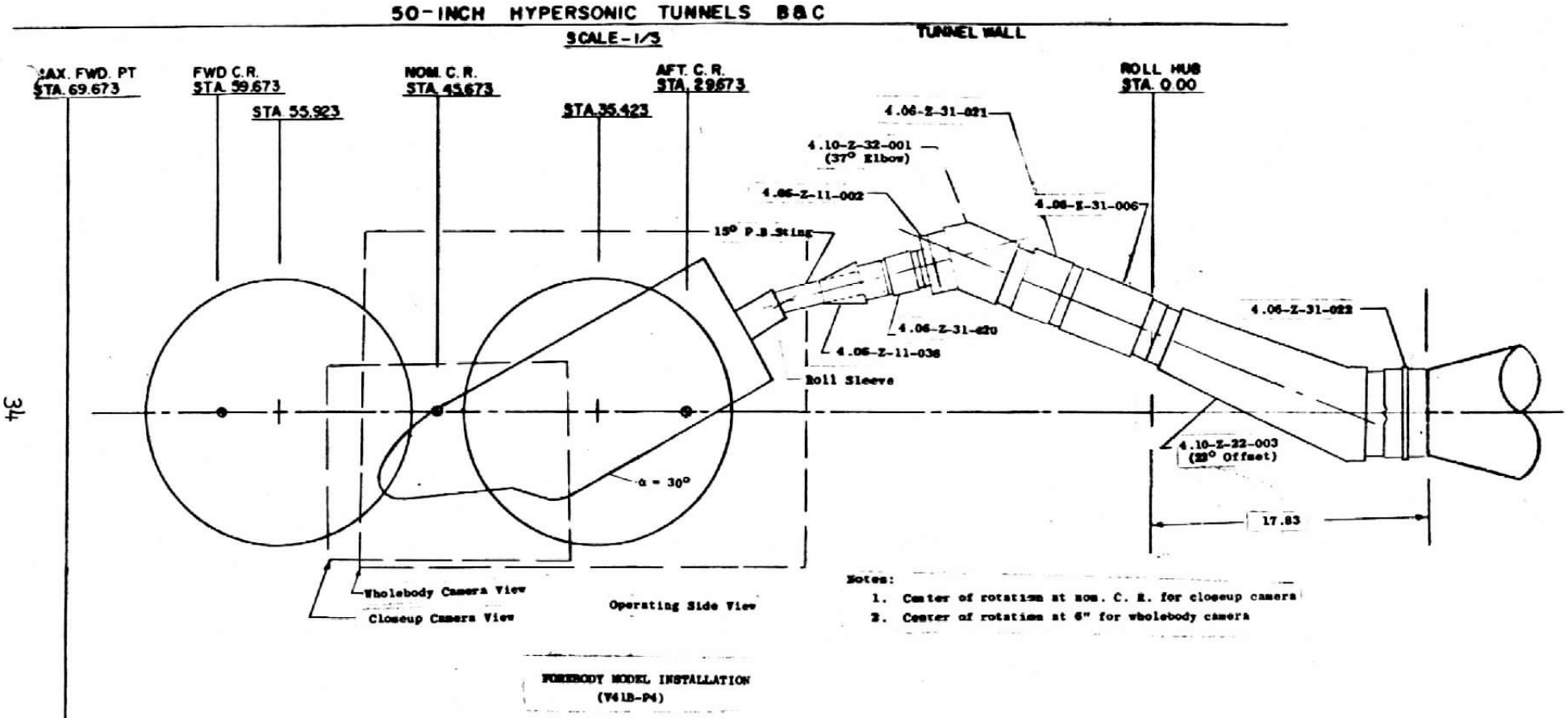

Figure 9. Forebody Model Installation Sketch

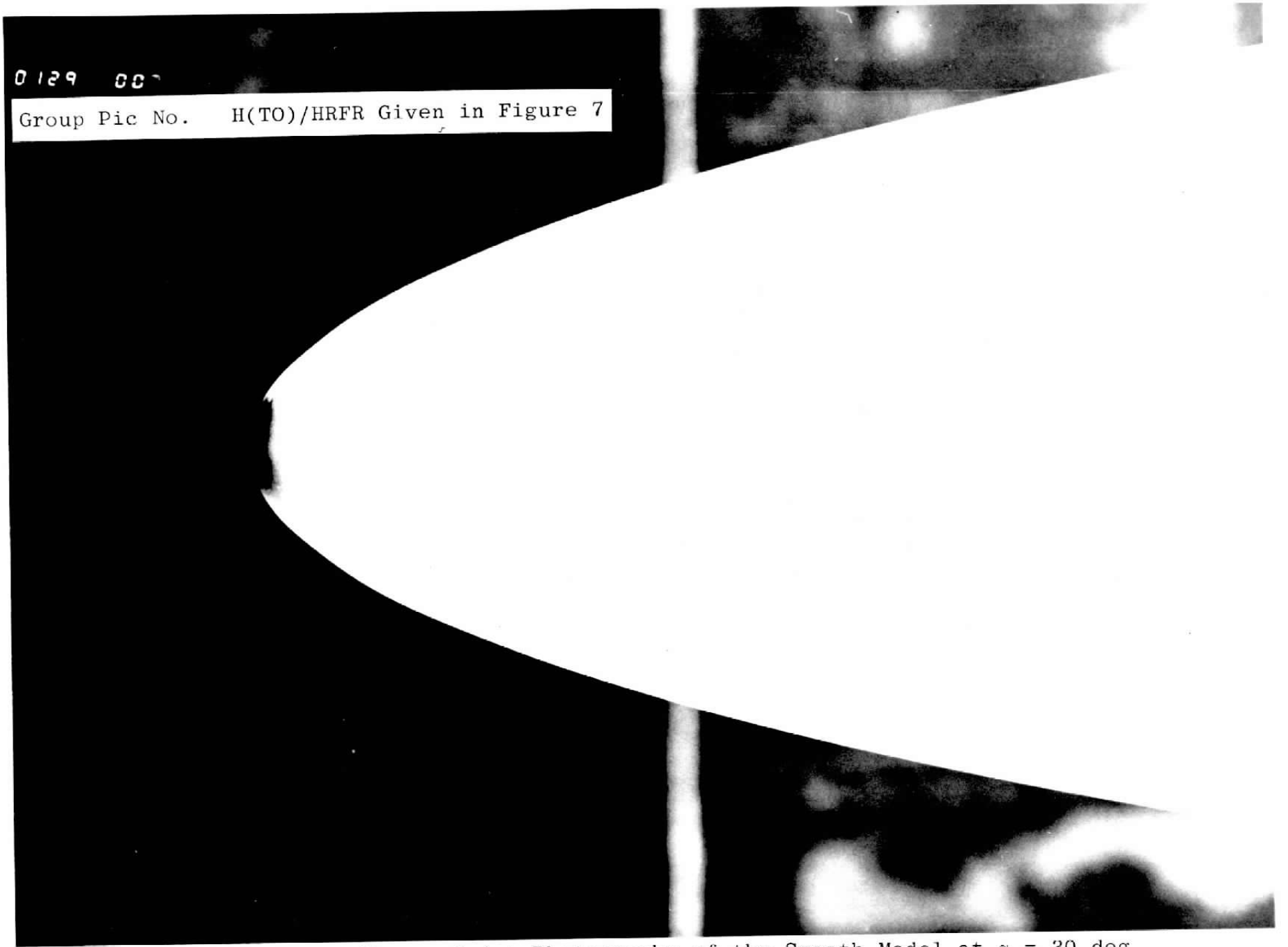

Figure 10. Phase-Change Paint Photographs of the Smooth Model at α = 30 deg (Group 129)

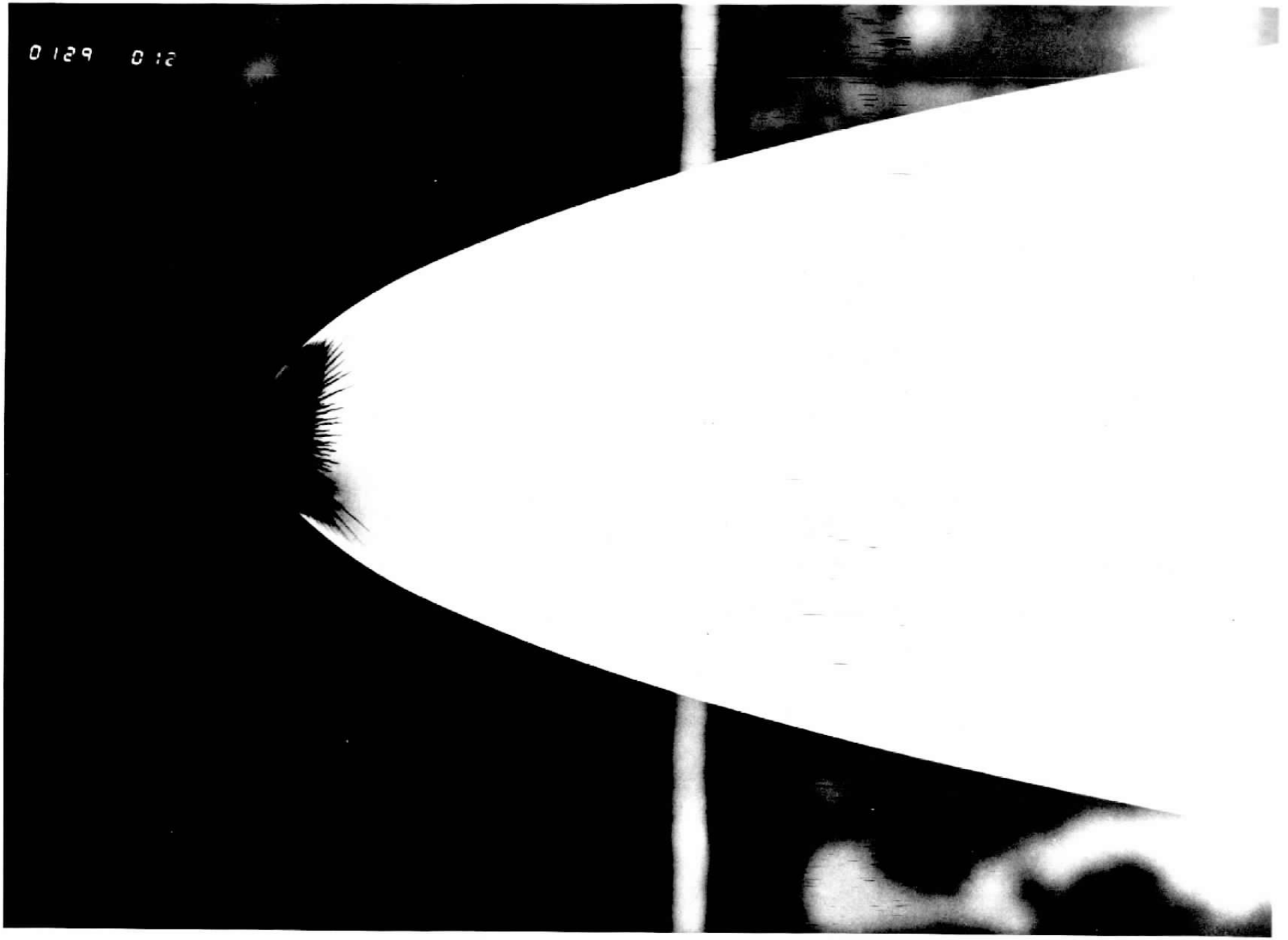

Figure 10. Continued

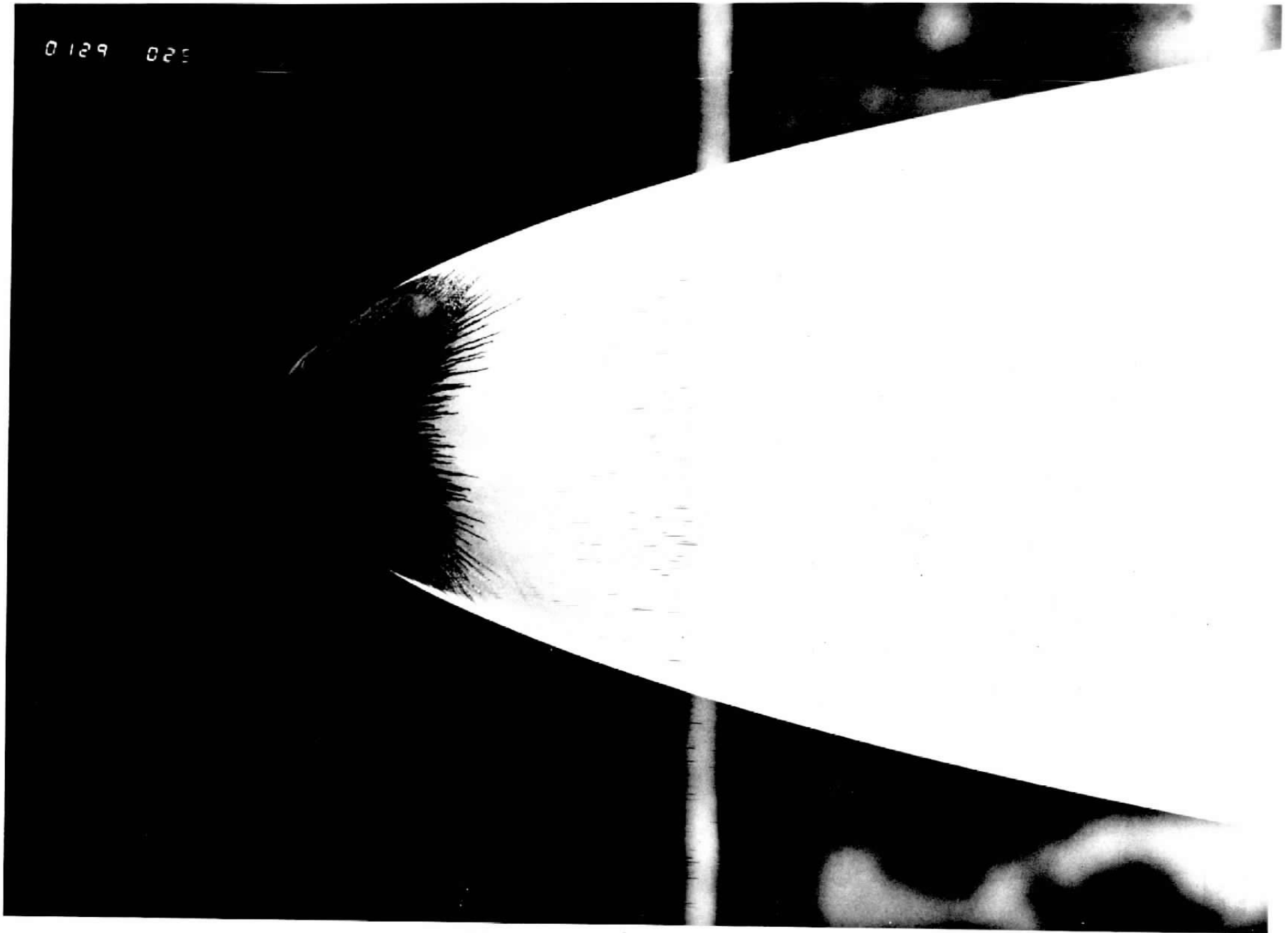

Figure 10. Concluded

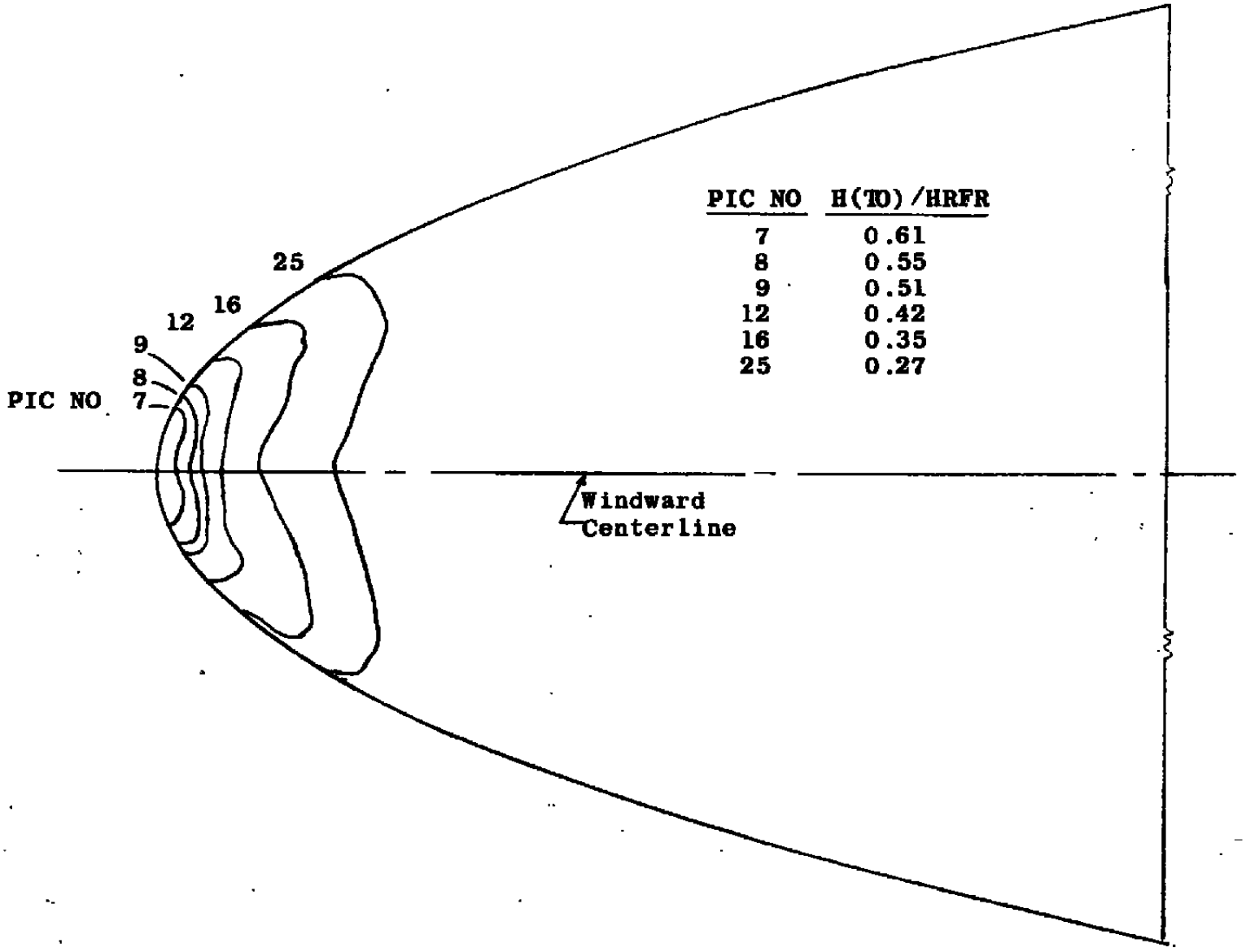

Figure 11. Tracings of the Melt Lines for the Smooth Model at α = 30 deg (Group 129)

[redacted]E [redacted]-78 [redacted]ECI [redacted]V418[redacted]

ARO, INC.
AEDC DIVISION
A SVERDRUP CORPORATION COMPANY
NASA RI OH90A INFRA-RED
ARNOLD AIR FORCE STATION TENNESSEE

GROUP 8002 DATA RECORDED 3-MAR-78 181 5:27:141 $\alpha = 30^{\circ}$

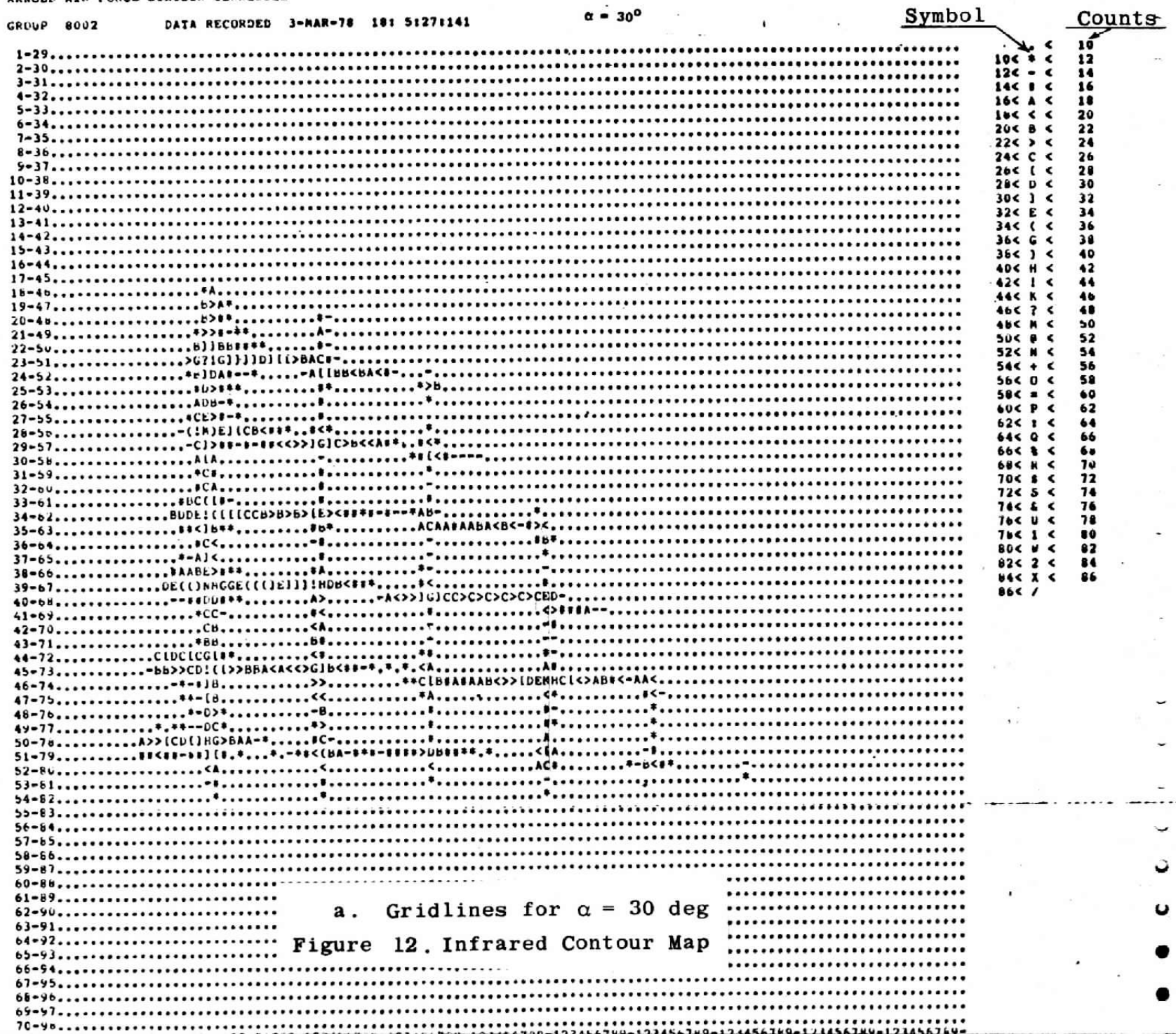

a. Gridlines for $\alpha = 30$ deg

Figure 12. Infrared Contour Map

[redacted]-MAR-78 [redacted]OJEC[redacted] V4[redacted]A
[redacted]RD, [redacted]
AEDC DIVISION
A SVERDRUP CORPORATION COMPANY
NASA RI UHYUA INFRA-RED
ARNOLD AIR FORCE STATION TENNESSEE

GROUP 6001 DATA RECORDED 3-MAR-78 17:38:22:517 $\alpha = 40^{\circ}$

Symbol		Counts
.	<	0
0< *	<	20
20< -	<	40
40< #	<	60
60< A	<	80
80< <	<	100
100< B	<	120
120< >	<	140
140< C	<	160
160< [	<	180
180< D	<	200
200<]	<	220
220< E	<	240
240< (	<	260
260< G	<	280
280<)	<	300
300< H	<	320
320< I	<	340
340< K	<	360
360< ?	<	380
380< M	<	400
400< @	<	420
420< N	<	440
440< +	<	460
460< O	<	480
480< =	<	500
500< P	<	520
520< :	<	540
540< Q	<	560
560< %	<	580
580< R	<	600
600< $	<	620
620< S	<	640
640< &	<	660
660< U	<	680
680< 1	<	700
700< W	<	720
720< 2	<	740
740< X	<	760
760< /		

1-29
2-30
3-31
4-32
5-33
6-34
7-35
8-36
9-37
10-38
11-39
12-40
13-41
14-42
15-43
16-44
17-45
18-46
19-47
20-48
21-49
22-50
23-51
24-52
25-53
26-54
27-55
28-56
29-57
30-58
31-59
32-60
33-61
34-62
35-63
36-64
37-65
38-66
39-67
40-68
41-69
42-70
43-71
44-72
45-73
46-74
47-75
48-76
49-77
50-78
51-79
52-80
53-81
54-82
55-83
56-84
57-85
58-86
59-87
60-88
61-89
62-90
63-91
64-92
65-93
66-94
67-95
68-96
69-97
70-98

123456789=123456789=123456789=123456789=123456789=123456789=123456789=123456789=123456789=123456789=123456789=

b. Gridlines for $\alpha = 40$ deg

Figure 12. Continued

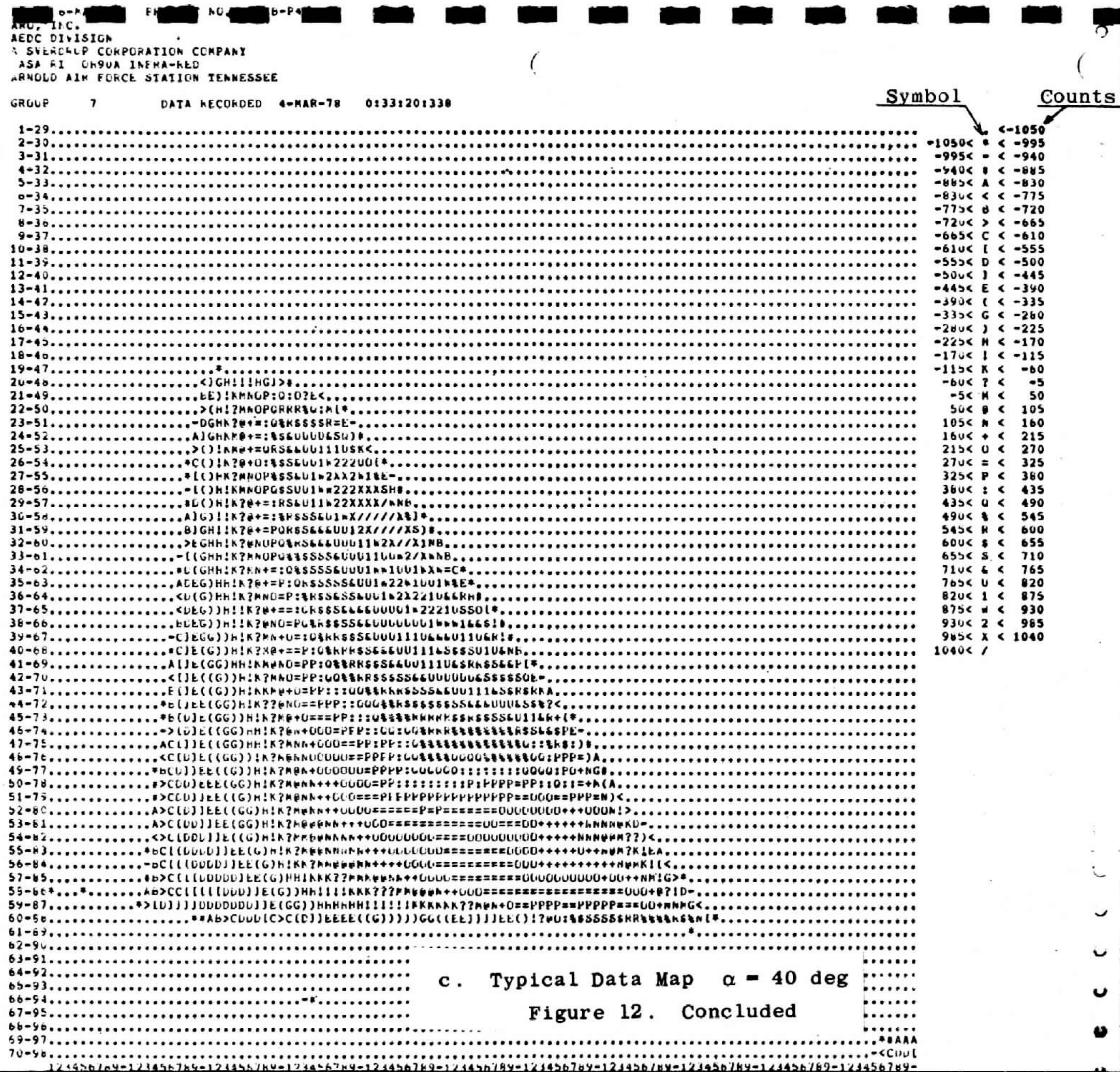

c. Typical Data Map α = 40 deg

Figure 12. Concluded

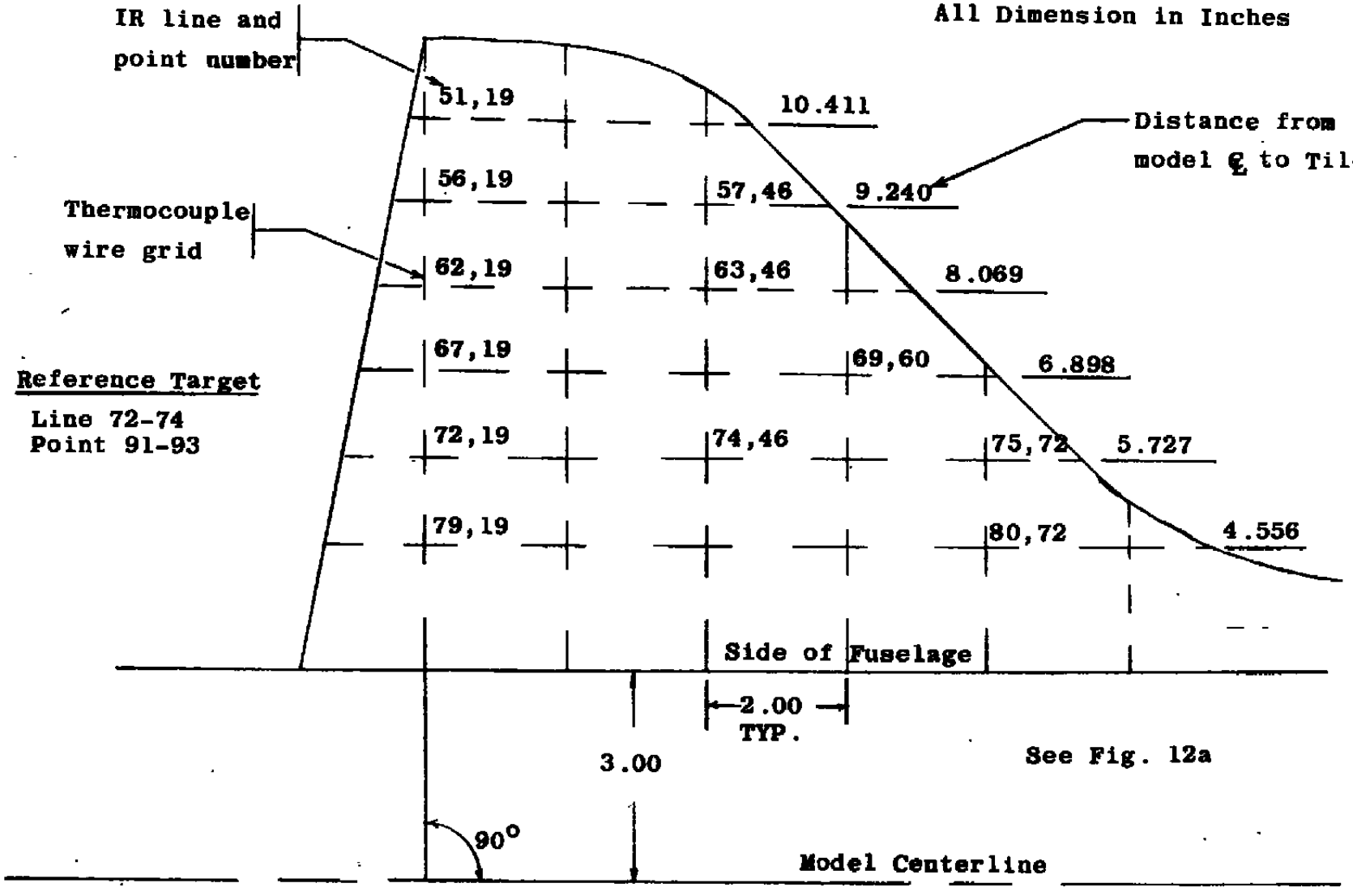

a. Tare Number 8002, ALPHA MODEL = 30°

Fig. 13 Gridline Layout for OH-90A Tare Photographs

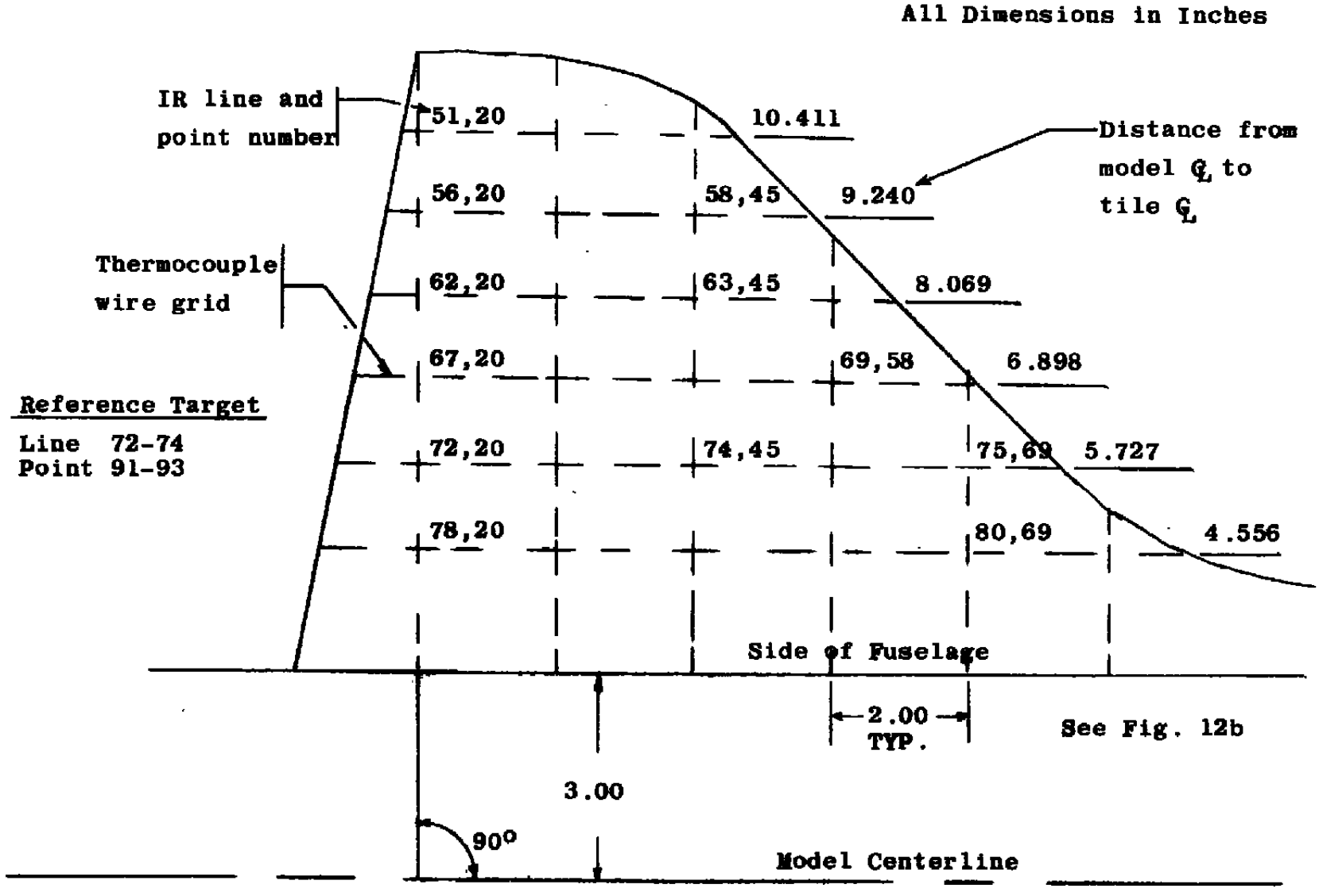

b. Tare Number 8001, ALPHA MODEL = 40°

Figure 13. Concluded

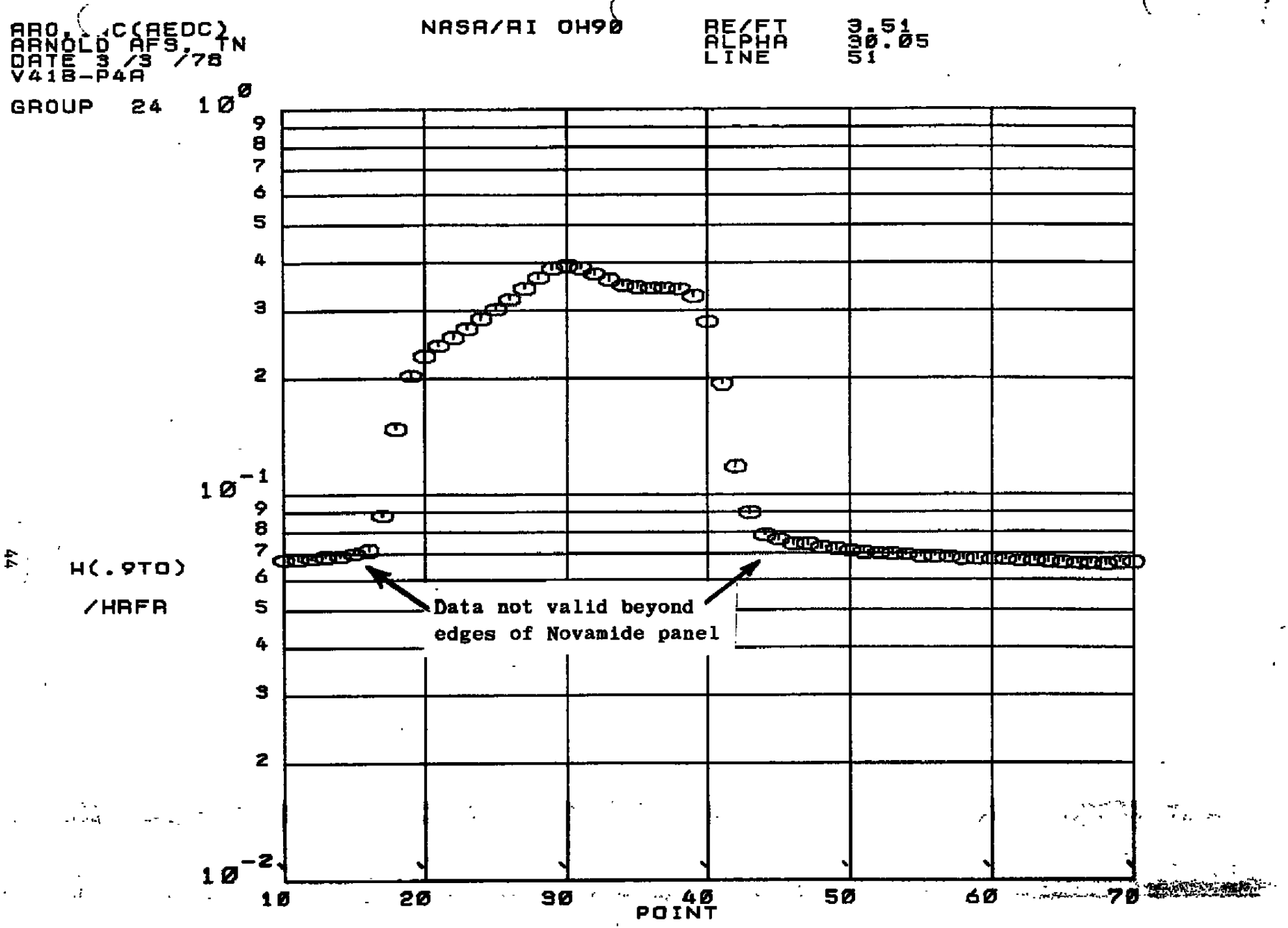

Figure 14. Sample IR Data Plot

	Test	RE/FT	Model Scale
△	OH-56	3.0×10^6	0.080
○	OH-90	3.5×10^6	0.025

Closed symbols are OH-90 data adjusted to match OH-56 scale (See Eqn. 6)

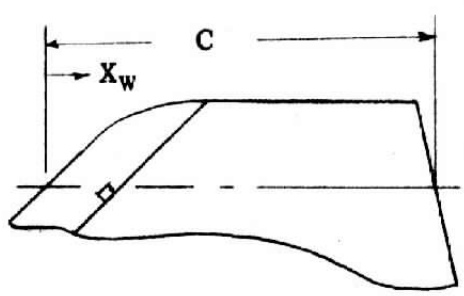

$M_\infty = 8.0$
$\alpha = 30^\circ$
$\frac{Y}{b/2} = 0.9$

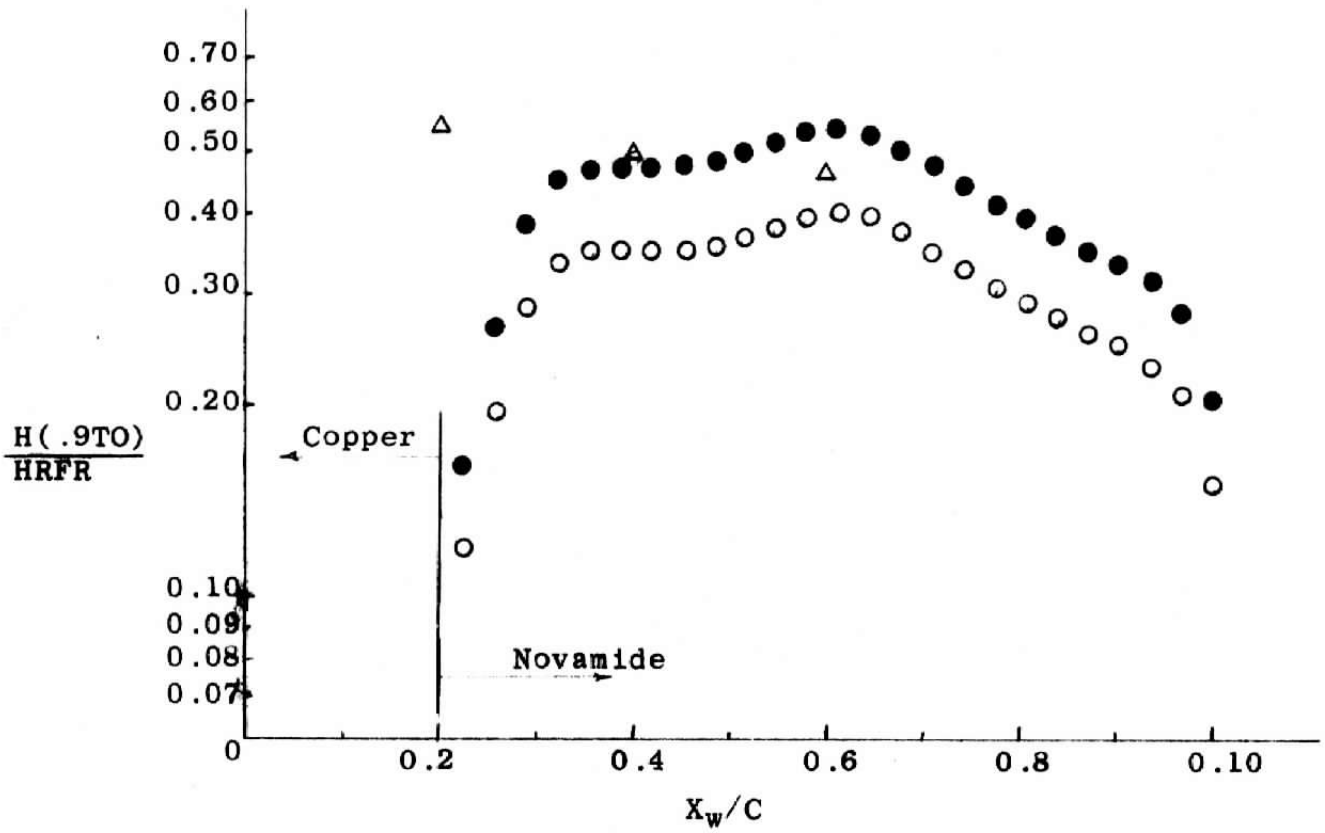

Figure 15. Comparison of IR Data with Previous Test Results

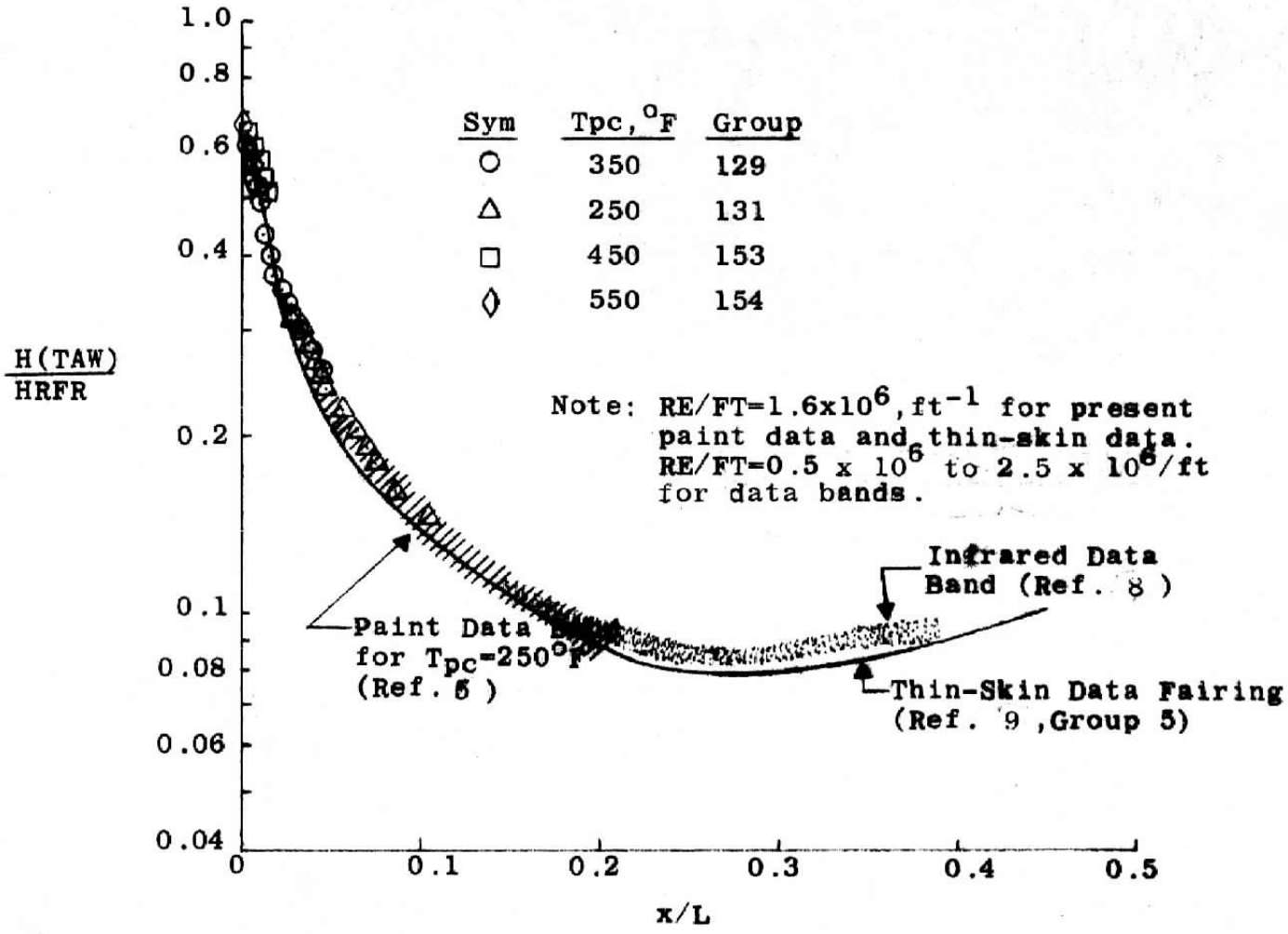

Figure 16. Comparison of Forebody Windward Centerline Data with Results from Previous Tests

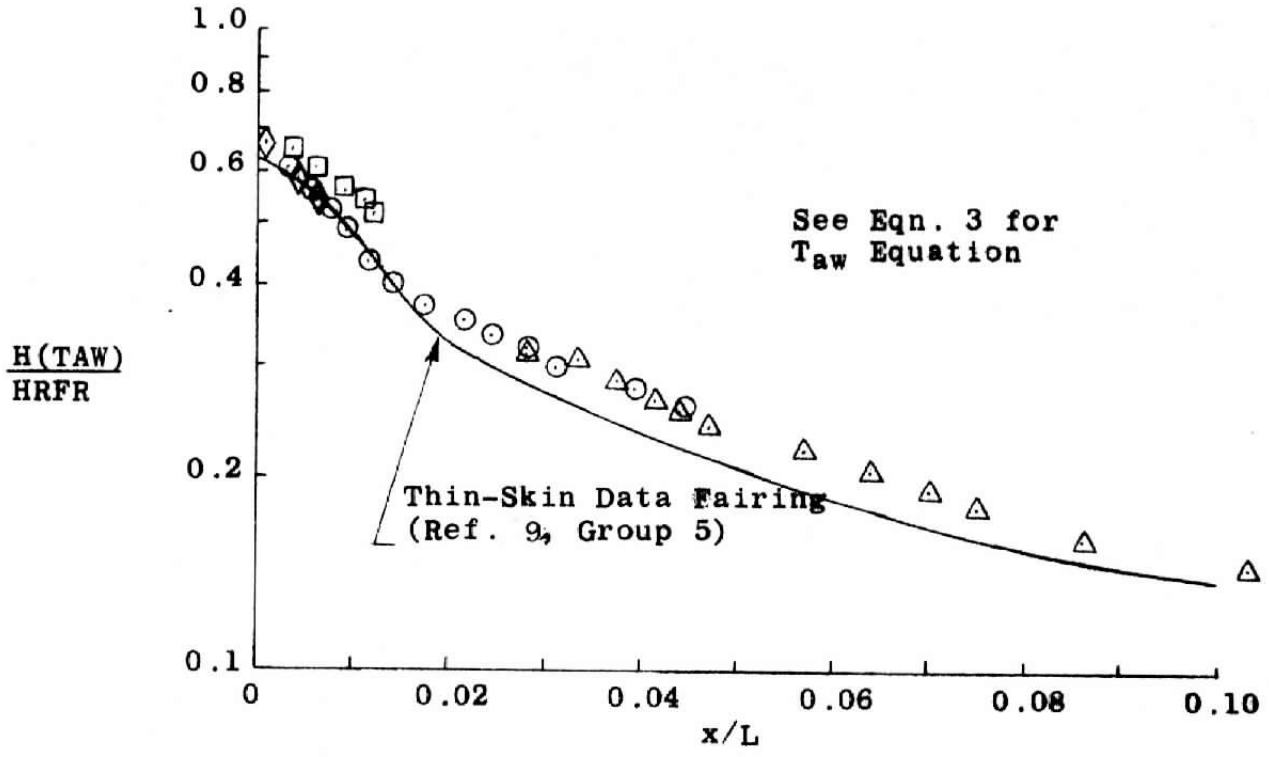

a. Computed Adiabatic Wall Temperature

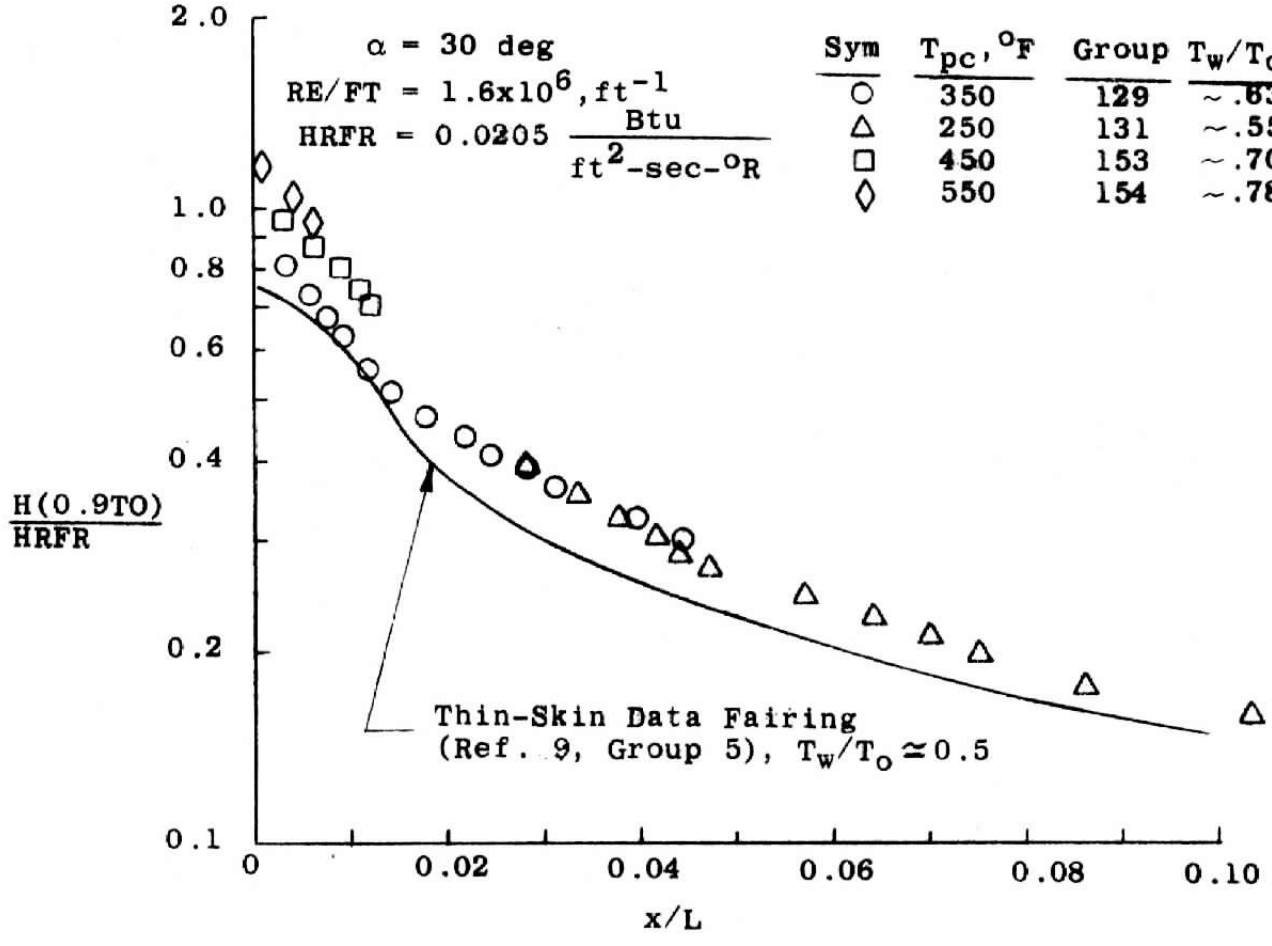

b. Assumed Adiabatic Wall Temperature = 0.9TO

Figure 17. Correlation of Windward Centerline Data Using a Computed Adiabatic Wall Temperature vs an Assumed Adiabatic Wall Temperature

V41B-P4A
ARO,INC. AEDC DIVISION
A SVERDRUP CORP. CO.
YKF ARNOLD AF STATION
50 INCH HYPERSONIC TUNNEL B

GROUP	CONFIG	MODEL DESCRIPTION	ALPHA-SECTOR DEG	ALPHA-MODEL DEG	ALPHA-MODEL-CORRECTED	PCK1/2	HR MIN SEC
129	1	0.04 FOREBODY-P6	0.32	29.68	29.99	0.0579	20 9 35

MACH	PO(PSIA)	TO(DEG R)	T-INF DEG R	P-INF PSIA	V-INF FT/SEC	RHO-INF SLUGS/FT3	MU-INF LB-SEC/FT2	RE/FT	HRFR BTU/FT2-SEC R	INITIAL TEMP DEG R
7.97	347.73	1291.67	94.25	0.0365	3793.	3.248E-05	7.585E-08	1.625E+06	2.067E-02	530.7

CAMERA	ROLL NO	PAINT TEMP(DEG F)	TBAR(TO)	BETA(TO)	TBAR(.9TO)	BETA(.9TO)
TOP	1859	350.	3.666E-01	4.663E-01	4.416E-01	6.213E-01
OS	1877	350.	3.666E-01	4.663E-01	4.416E-01	6.213E-01

PIC	NO	TIME	DELTIME	H(TO)	H(TO)/HRFR	H(.9TO)	H(.9TO)/HRFR
TOP	1(350)	0.19		MODEL HAS NOT REACHED CENTERLINE			
OS	1(350)	0.19		MODEL HAS NOT REACHED CENTERLINE			
TOP	2(350)	1.23		MODEL HAS NOT REACHED CENTERLINE			
OS	2(350)	1.23		MODEL HAS NOT REACHED CENTERLINE			
TOP	3(350)	2.26		MODEL HAS NOT REACHED CENTERLINE			
OS	3(350)	2.26		MODEL HAS NOT REACHED CENTERLINE			
INJECT TIME =		3.24					
TOP	4(350)	3.29	1.47	2.226E-02	1.0767	2.965E-02	1.4345
OS	4(350)	3.29	1.47	2.226E-02	1.0767	2.965E-02	1.4345
TOP	5(350)	4.32	2.50	1.706E-02	0.8255	2.273E-02	1.0998
OS	5(350)	4.32	2.50	1.706E-02	0.8255	2.273E-02	1.0998
TOP	6(350)	5.35	3.54	1.436E-02	0.6946	1.913E-02	0.9254
OS	6(350)	5.35	3.54	1.436E-02	0.6946	1.913E-02	0.9254
TOP	7(350)	6.39	4.57	1.263E-02	0.6111	1.683E-02	0.8142
OS	7(350)	6.39	4.57	1.263E-02	0.6111	1.683E-02	0.8142
TOP	8(350)	7.42	5.60	1.141E-02	0.5520	1.520E-02	0.7354
OS	8(350)	7.42	5.60	1.141E-02	0.5520	1.520E-02	0.7354
TOP	9(350)	8.45	6.63	1.048E-02	0.5072	1.397E-02	0.6757
OS	9(350)	8.45	6.63	1.048E-02	0.5072	1.397E-02	0.6757
TOP	10(350)	9.48	7.66	9.752E-03	0.4718	1.299E-02	0.6286
OS	10(350)	9.48	7.66	9.752E-03	0.4718	1.299E-02	0.6286
TOP	11(350)	10.51	8.70	9.155E-03	0.4429	1.220E-02	0.5901
OS	11(350)	10.51	8.70	9.155E-03	0.4429	1.220E-02	0.5901
TOP	12(350)	11.55	9.73	8.656E-03	0.4188	1.153E-02	0.5579
OS	12(350)	11.55	9.73	8.656E-03	0.4188	1.153E-02	0.5579
TOP	13(350)	12.58	10.76	8.231E-03	0.3982	1.097E-02	0.5305
OS	13(350)	12.58	10.76	8.231E-03	0.3982	1.097E-02	0.5305
TOP	14(350)	13.61	11.79	7.862E-03	0.3804	1.047E-02	0.5067
OS	14(350)	13.61	11.79	7.862E-03	0.3804	1.047E-02	0.5067
TOP	15(350)	14.64	12.83	7.539E-03	0.3647	1.004E-02	0.4859
OS	15(350)	14.64	12.83	7.539E-03	0.3647	1.004E-02	0.4859
TOP	16(350)	15.68	13.86	7.253E-03	0.3509	9.663E-03	0.4675
OS	16(350)	15.68	13.86	7.253E-03	0.3509	9.663E-03	0.4675
TOP	17(350)	16.71	14.89	6.997E-03	0.3385	9.322E-03	0.4510
OS	17(350)	16.71	14.89	6.997E-03	0.3385	9.322E-03	0.4510

a. Phase-Change Paint Data

Figure 18. Typical Data Tabulations

V411
ARO, INC. AEDC DIVISION
A SVERDRUP CORP. CO.
VKF ARNOLD AF STATION
50 INCH HYPERSONIC TUNNEL B

GROUP	CONFIG	MODEL DESCRIPTION	ALPHA-SECTOR DEG	ALPHA-MODEL DEG	ALPHA-MODEL-CORRECTED	PCK1/2	HR MIN SEC
129	1	0.04 FOREBODY-P8	0.32	29.68	29.99	0.0579	20 9 35

MACH	PO(PSIA)	TO(DEG R)	T-INF DEG R	P-INF PSIA	V-INF FT/SEC	RHO-INF SLUGS/FT3	MU-INF LB-SEC/FT2	RE/FT	HRFR BTU/FT2-SEC R	INITIAL TEMP DEG R
7.97	347.73	1291.67	94.25	0.0365	3793.	3.248E-05	7.585E-08	1.625E+06	2.067E-02	530.7

CAMERA	ROLL NO	PAINT TEMP(DEG F)	TBAR(TO)	BETA(TO)	TBAR(.9TO)	BETA(.9TO)
TOP	1859	350.	3.666E-01	4.663E-01	4.416E-01	6.213E-01
OS	1877	350.	3.666E-01	4.663E-01	4.416E-01	6.213E-01

PIC NO		TIME	DELTIME	H(TO)	H(TO)/ HRFR	H(.9TO)	H(.9TO)/ HRFR
TOP	18(350)	17.74	15.92	6.766E-03	0.3273	9.015E-03	0.4361
OS	18(350)	17.74	15.92	6.766E-03	0.3273	9.015E-03	0.4361
TOP	19(350)	18.77	16.95	6.557E-03	0.3172	8.736E-03	0.4226
OS	19(350)	18.77	16.95	6.557E-03	0.3172	8.736E-03	0.4226
TOP	20(350)	19.80	17.99	6.366E-03	0.3080	8.482E-03	0.4103
OS	20(350)	19.80	17.99	6.366E-03	0.3080	8.482E-03	0.4103
TOP	21(350)	20.84	19.02	6.191E-03	0.2995	8.248E-03	0.3990
OS	21(350)	20.84	19.02	6.191E-03	0.2995	8.248E-03	0.3990
TOP	22(350)	21.87	20.05	6.030E-03	0.2917	8.033E-03	0.3886
OS	22(350)	21.87	20.05	6.030E-03	0.2917	8.033E-03	0.3886
TOP	23(350)	22.90	21.08	5.880E-03	0.2845	7.834E-03	0.3790
OS	23(350)	22.90	21.08	5.880E-03	0.2845	7.834E-03	0.3790
TOP	24(350)	23.93	22.12	5.741E-03	0.2778	7.649E-03	0.3701
OS	24(350)	23.93	22.12	5.741E-03	0.2778	7.649E-03	0.3701
TOP	25(350)	24.97	23.15	5.612E-03	0.2715	7.477E-03	0.3617
OS	25(350)	24.97	23.15	5.612E-03	0.2715	7.477E-03	0.3617
TOP	26(350)	26.00	24.18	5.491E-03	0.2656	7.315E-03	0.3539
OS	26(350)	26.00	24.18	5.491E-03	0.2656	7.315E-03	0.3539
TOP	27(350)	27.03	25.21	5.377E-03	0.2601	7.164E-03	0.3466
OS	27(350)	27.03	25.21	5.377E-03	0.2601	7.164E-03	0.3466
TOP	28(350)	28.06	26.24	5.270E-03	0.2550	7.022E-03	0.3397
OS	28(350)	28.06	26.24	5.270E-03	0.2550	7.022E-03	0.3397
TOP	29(350)	29.09	27.28	5.170E-03	0.2501	6.888E-03	0.3332
OS	29(350)	29.09	27.28	5.170E-03	0.2501	6.888E-03	0.3332
TOP	30(350)	30.13	28.31	5.075E-03	0.2455	6.761E-03	0.3271
OS	30(350)	30.13	28.31	5.075E-03	0.2455	6.761E-03	0.3271
TOP	31(350)	31.16	29.34	4.985E-03	0.2411	6.641E-03	0.3213
OS	31(350)	31.16	29.34	4.985E-03	0.2411	6.641E-03	0.3213
TOP	32(350)	32.19	30.37	4.899E-03	0.2370	6.527E-03	0.3158
OS	32(350)	32.19	30.37	4.899E-03	0.2370	6.527E-03	0.3158
TOP	33(350)	33.22	31.40	4.818E-03	0.2331	6.419E-03	0.3105
OS	33(350)	33.22	31.40	4.818E-03	0.2331	6.419E-03	0.3105
TOP	34(350)	34.25	32.44	4.741E-03	0.2293	6.316E-03	0.3056
OS	34(350)	34.25	32.44	4.741E-03	0.2293	6.316E-03	0.3056

Figure 16. Continued

NASA. H90 TRANSITION TEST
V41B-R4A
ARO,INC. AEDC DIVISION
A SVERDRUP CORP. CO.
VKF ARNOLD AF STATION
50 INCH HYPERSONIC TUNNEL 8

GROUP	CONFIG	MODEL DESCRIPTION	ALPHA-SECTOR DEG	ALPHA-MODEL DEG	ALPHA-MODEL-CORRECTED	PCK1/2	HR MIN SEC
129	1	0.04 FOREBODY-P8	0.32	29.68	29.99	0.0579	20 9 35

MACH	PO(PSIA)	TO(DEG R)	T-INF DEG R	P-INF PSIA	V-INF FT/SEC	RHO-INF SLUGS/FT3	MU-INF LB-SEC/FT2	RE/FT	HRFR BTU/FT2-SEC R	INITIAL TEMP DEG R
7.97	347.73	1291.67	94.25	0.0365	3793.	3.248E-05	7.585E-08	1.625E+06	2.067E-02	530.7

CAMERA	ROLL NO	PAINT TEMP(DEG F)	TBAR(TO)	BETA(TO)	TBAR(.9TO)	BETA(.9TO)
TOP	1859	350.	3.666E-01	4.663E-01	4.416E-01	6.213E-01
OS	1877	350.	3.666E-01	4.663E-01	4.416E-01	6.213E-01

PIC NO		TIME	DELTIME	H(TO)	H(TO)/ HRFR	H(.9TO)	H(.9TO)/ HRFR
TOP	35(350)	35.29	33.47	4.667E-03	0.2258	6.218E-03	0.3008
OS	35(350)	35.29	33.47	4.667E-03	0.2258	6.218E-03	0.3008
TOP	36(350)	36.32	34.50	4.597E-03	0.2224	6.124E-03	0.2963
OS	36(350)	36.32	34.50	4.597E-03	0.2224	6.124E-03	0.2963
TOP	37(350)	37.35	35.53	4.529E-03	0.2191	6.035E-03	0.2919
OS	37(350)	37.35	35.53	4.529E-03	0.2191	6.035E-03	0.2919
TOP	38(350)	38.38	36.57	4.465E-03	0.2160	5.949E-03	0.2878
OS	38(350)	38.38	36.57	4.465E-03	0.2160	5.949E-03	0.2878
TOP	39(350)	39.42	37.60	4.403E-03	0.2130	5.867E-03	0.2838
OS	39(350)	39.42	37.60	4.403E-03	0.2130	5.867E-03	0.2838
TOP	40(350)	40.45	38.63	4.344E-03	0.2102	5.788E-03	0.2800
OS	40(350)	40.45	38.63	4.344E-03	0.2102	5.788E-03	0.2800
TOP	41(350)	41.48	39.66	4.287E-03	0.2074	5.712E-03	0.2763
OS	41(350)	41.48	39.66	4.287E-03	0.2074	5.712E-03	0.2763

Figure 18. Continued

NASA/RI OH90 TRANSITION TEST
V41B-P4A
ARO, INC. AEDC DIVISION
A SVERDRUP CORP. CO.
VKF ARNOLD AF STATION
50 INCH HYPERSONIC TUNNEL B

MAR 3,1978

GROUP	* * * * TITLE TYPE	MODEL DESCRIPTION * * * * GAP	HEIGHT	ALPHA-SECTOR DEG	ALPHA-MODEL DEG	PCK1/2	HR	MIN	SEC
2	KSI FORWARD	0.01	0.000	0.01	29.99	0.053	21.	46	1

MACH	PO(PSIA)	TO(DEG R)	T-INF DEG R	P-INF PSIA	V-INF FT/SEC	RHO-INF SLUGS/FT3	MU-INF LB-SEC/FT2	RE/F FT-1	HRFR BTU/FT2-SEC-R	INITIAL TEMP DEG R
7.99	553.15	1321.67	96.00	0.0571	3638.	0.100E+04	0.773E-07	0.248E+07	0.331E-01	526.7

IR CAMERA INFORMATION

MOUNTING LOCATION	260
F STOP	1.8
LENS-DEG	15
SENSITIVITY	1000.
BLACK LEVEL VOLTAGE	2.4542
LINE SCAN PHI	90
MODEL EMISSIVITY	0.96
REF EMISSIVITY	0.94
WINDOW FACTOR	0.860

TIME RECORDS

LIFT OFF	0.00
CENTER LINE	1.00
IR SCAN TIME	9.95
DELTA TIME,SEC	9.39
PHOTO 1 TIME	2146
PHOTO 2 TIME	0
PHOTO 3 TIME	0
PHOTO 4 TIME	0

REFERENCE TARGET INFORMATION

TCR5	500.61
TCR6	-228.49
POINT	0
LINE	-1287

DIGITAL DATA AREA PRINTOUT LOCATION

LINE 29 THROUGH 98

POINT 1 THROUGH 110

b. Infrared Data

Figure 18. Continued

IR TEMPERATURE RECORD -- TWALL/INITIAL TEMP

GROUP 2

IR SCAN TIME 9.39 SEC
INITIAL TEMP 526.7 DEG. R

*** POINT ***

LINE	1	2	3	4	5	6	7	8	9	10	11	12	13	14	15	16	17	18	19	20
29	1.088	1.092	1.095	1.097	1.101	1.097	1.098	1.097	1.096	1.095	1.095	1.094	1.092	1.093	1.093	1.093	1.090	1.095	1.096	1.095
30	1.094	1.097	1.100	1.099	1.100	1.098	1.096	1.095	1.096	1.094	1.093	1.093	1.094	1.094	1.095	1.095	1.097	1.097	1.097	1.096
31	1.100	1.101	1.101	1.101	1.097	1.096	1.094	1.097	1.097	1.098	1.097	1.098	1.096	1.097	1.097	1.099	1.098	1.100	1.097	1.097
32	1.103	1.102	1.101	1.098	1.099	1.097	1.100	1.099	1.099	1.099	1.099	1.099	1.100	1.101	1.100	1.099	1.099	1.098	1.097	1.095
33	1.102	1.100	1.101	1.101	1.102	1.102	1.103	1.102	1.101	1.100	1.101	1.101	1.101	1.099	1.098	1.097	1.097	1.095	1.095	1.093
34	1.102	1.103	1.103	1.103	1.106	1.105	1.103	1.101	1.102	1.101	1.101	1.098	1.098	1.096	1.095	1.095	1.095	1.096	1.099	1.101
35	1.107	1.103	1.106	1.100	1.101	1.098	1.101	1.095	1.097	1.094	1.096	1.091	1.093	1.091	1.096	1.100	1.102	1.103	1.104	1.105
36	1.107	1.105	1.103	1.103	1.100	1.099	1.096	1.096	1.092	1.095	1.094	1.097	1.097	1.100	1.100	1.103	1.104	1.106	1.104	1.105
37	1.103	1.100	1.100	1.097	1.094	1.092	1.093	1.094	1.097	1.097	1.099	1.099	1.102	1.103	1.105	1.104	1.103	1.098	1.093	1.081
38	1.097	1.095	1.092	1.093	1.093	1.096	1.097	1.100	1.100	1.102	1.100	1.103	1.103	1.105	1.098	1.092	1.080	1.071	1.057	1.050
39	1.093	1.093	1.096	1.097	1.098	1.099	1.101	1.101	1.102	1.103	1.103	1.099	1.094	1.084	1.075	1.060	1.051	1.047	1.049	1.047
40	1.095	1.097	1.098	1.101	1.100	1.103	1.101	1.105	1.102	1.096	1.086	1.077	1.062	1.056	1.050	1.051	1.050	1.049	1.047	1.050
41	1.100	1.101	1.102	1.102	1.103	1.103	1.102	1.092	1.063	1.068	1.061	1.054	1.051	1.050	1.051	1.050	1.050	1.050	1.051	1.053
42	1.105	1.103	1.106	1.102	1.100	1.086	1.078	1.060	1.056	1.050	1.051	1.049	1.053	1.053	1.053	1.050	1.053	1.051	1.054	1.053
43	1.110	1.109	1.104	1.091	1.077	1.061	1.057	1.053	1.053	1.051	1.056	1.053	1.054	1.053	1.054	1.053	1.056	1.050	1.054	1.051
44	1.105	1.092	1.076	1.065	1.060	1.060	1.054	1.056	1.053	1.057	1.054	1.060	1.058	1.060	1.057	1.060	1.054	1.060	1.060	1.062
45	1.079	1.068	1.065	1.061	1.061	1.058	1.061	1.060	1.061	1.060	1.061	1.060	1.063	1.060	1.065	1.063	1.066	1.063	1.066	1.066
46	1.071	1.068	1.066	1.070	1.065	1.067	1.063	1.066	1.065	1.067	1.066	1.070	1.066	1.070	1.070	1.073	1.072	1.080	1.093	1.110
47	1.076	1.073	1.073	1.072	1.073	1.072	1.073	1.071	1.072	1.071	1.075	1.073	1.075	1.075	1.078	1.078	1.084	1.116	1.193	1.256
48	1.078	1.077	1.078	1.079	1.077	1.078	1.077	1.078	1.077	1.079	1.078	1.080	1.080	1.084	1.084	1.086	1.091	1.140	1.240	1.317
49	1.083	1.083	1.081	1.079	1.083	1.080	1.083	1.079	1.080	1.079	1.084	1.084	1.085	1.085	1.087	1.089	1.099	1.152	1.261	1.340
50	1.083	1.083	1.085	1.084	1.086	1.084	1.085	1.083	1.085	1.085	1.086	1.085	1.087	1.085	1.090	1.090	1.105	1.174	1.289	1.361
51	1.085	1.085	1.085	1.083	1.086	1.083	1.087	1.085	1.087	1.085	1.087	1.087	1.090	1.091	1.095	1.096	1.122	1.222	1.330	1.388
52	1.081	1.080	1.079	1.081	1.080	1.084	1.081	1.085	1.083	1.085	1.084	1.087	1.087	1.090	1.091	1.099	1.140	1.258	1.354	1.404
53	1.075	1.075	1.076	1.073	1.075	1.072	1.073	1.073	1.077	1.076	1.078	1.078	1.081	1.081	1.085	1.093	1.160	1.281	1.364	1.404
54	1.061	1.062	1.062	1.063	1.062	1.063	1.060	1.065	1.061	1.065	1.063	1.068	1.067	1.072	1.073	1.094	1.185	1.303	1.367	1.400
55	1.053	1.051	1.053	1.050	1.051	1.050	1.051	1.053	1.054	1.054	1.060	1.060	1.060	1.060	1.065	1.093	1.206	1.316	1.371	1.397
56	1.050	1.043	1.043	1.044	1.046	1.047	1.047	1.049	1.049	1.049	1.050	1.051	1.051	1.060	1.066	1.098	1.217	1.318	1.368	1.393
57	1.046	1.044	1.044	1.043	1.044	1.043	1.044	1.046	1.049	1.050	1.051	1.050	1.053	1.053	1.063	1.103	1.225	1.319	1.364	1.386
58	1.043	1.041	1.043	1.041	1.043	1.043	1.043	1.041	1.044	1.046	1.049	1.047	1.053	1.056	1.065	1.121	1.245	1.326	1.364	1.384
59	1.040	1.038	1.040	1.040	1.040	1.038	1.038	1.040	1.041	1.041	1.046	1.046	1.049	1.051	1.070	1.159	1.276	1.338	1.367	1.384
60	1.038	1.035	1.035	1.037	1.037	1.038	1.033	1.038	1.037	1.041	1.041	1.043	1.043	1.049	1.075	1.186	1.294	1.345	1.368	1.384
61	1.037	1.035	1.035	1.033	1.033	1.033	1.037	1.033	1.037	1.037	1.040	1.040	1.041	1.047	1.094	1.224	1.319	1.359	1.379	1.392
62	1.035	1.033	1.032	1.037	1.033	1.035	1.033	1.035	1.037	1.040	1.040	1.043	1.044	1.054	1.126	1.258	1.334	1.368	1.388	1.402
63	1.035	1.033	1.033	1.030	1.033	1.030	1.035	1.033	1.038	1.038	1.041	1.041	1.044	1.056	1.151	1.275	1.340	1.370	1.389	1.403

Figure 18. Continued

IR HEAT TRANSFER COEFFICIENT = H(,9IO)/HRFR
IR SCAN TIME 9.39 SEC
GROUP 2 HRFR = 0.331E-01

*** POINT ***

LINE	1	2	3	4	5	6	7	8	9	10	11	12	13	14	15	16	17	18	19	20
29	0.034	0.036	0.037	0.038	0.040	0.038	0.039	0.038	0.038	0.037	0.037	0.037	0.036	0.037	0.037	0.037	0.035	0.037	0.038	0.037
30	0.037	0.038	0.040	0.039	0.040	0.039	0.038	0.037	0.038	0.037	0.037	0.037	0.037	0.037	0.037	0.037	0.037	0.038	0.038	0.038	0.038
31	0.040	0.040	0.040	0.040	0.038	0.038	0.037	0.038	0.038	0.039	0.038	0.039	0.038	0.038	0.038	0.039	0.039	0.040	0.038	0.038
32	0.041	0.040	0.040	0.039	0.039	0.038	0.040	0.039	0.039	0.039	0.039	0.039	0.040	0.040	0.040	0.039	0.039	0.039	0.038	0.037
33	0.040	0.040	0.040	0.040	0.040	0.040	0.041	0.040	0.040	0.040	0.040	0.040	0.040	0.039	0.039	0.038	0.038	0.037	0.037	0.037
34	0.040	0.041	0.041	0.041	0.042	0.042	0.041	0.040	0.040	0.040	0.040	0.039	0.039	0.038	0.037	0.037	0.037	0.038	0.039	0.040
35	0.042	0.041	0.042	0.040	0.040	0.039	0.040	0.037	0.038	0.037	0.038	0.036	0.037	0.036	0.038	0.040	0.040	0.041	0.041	0.042
36	0.042	0.042	0.041	0.041	0.040	0.039	0.038	0.038	0.036	0.037	0.037	0.038	0.038	0.040	0.040	0.041	0.041	0.042	0.041	0.042
37	0.041	0.040	0.040	0.038	0.037	0.036	0.037	0.037	0.038	0.038	0.039	0.039	0.040	0.041	0.042	0.041	0.041	0.039	0.037	0.032
38	0.038	0.037	0.036	0.037	0.037	0.038	0.038	0.040	0.040	0.040	0.040	0.041	0.041	0.042	0.039	0.036	0.031	0.027	0.022	0.019
39	0.037	0.037	0.038	0.038	0.039	0.039	0.040	0.040	0.040	0.041	0.041	0.039	0.037	0.033	0.029	0.023	0.020	0.018	0.019	0.018
40	0.037	0.038	0.039	0.040	0.040	0.041	0.040	0.042	0.040	0.038	0.034	0.030	0.024	0.021	0.019	0.020	0.019	0.019	0.018	0.019
41	0.040	0.040	0.040	0.040	0.041	0.041	0.040	0.036	0.032	0.026	0.023	0.021	0.020	0.019	0.020	0.019	0.019	0.019	0.020	0.020
42	0.042	0.041	0.042	0.040	0.040	0.034	0.030	0.023	0.021	0.019	0.020	0.019	0.020	0.020	0.020	0.019	0.020	0.020	0.021	0.020
43	0.044	0.043	0.041	0.036	0.030	0.023	0.022	0.020	0.020	0.020	0.021	0.020	0.021	0.020	0.021	0.020	0.021	0.019	0.021	0.020
44	0.042	0.036	0.029	0.025	0.023	0.023	0.021	0.021	0.020	0.022	0.021	0.023	0.022	0.023	0.022	0.023	0.021	0.023	0.023	0.024
45	0.031	0.026	0.025	0.023	0.023	0.022	0.023	0.023	0.023	0.023	0.023	0.023	0.024	0.023	0.025	0.024	0.025	0.024	0.025	0.025
46	0.027	0.026	0.025	0.027	0.025	0.026	0.024	0.025	0.025	0.026	0.025	0.027	0.025	0.027	0.027	0.028	0.028	0.031	0.037	0.044
47	0.029	0.028	0.028	0.028	0.028	0.028	0.028	0.027	0.028	0.027	0.029	0.028	0.029	0.029	0.030	0.030	0.033	0.046	0.081	0.113
48	0.030	0.030	0.030	0.031	0.030	0.030	0.030	0.030	0.030	0.031	0.030	0.031	0.031	0.033	0.033	0.034	0.036	0.057	0.105	0.147
49	0.032	0.032	0.032	0.031	0.032	0.031	0.032	0.031	0.031	0.031	0.033	0.033	0.033	0.033	0.034	0.035	0.039	0.062	0.116	0.161
50	0.032	0.032	0.033	0.033	0.034	0.033	0.033	0.032	0.033	0.033	0.034	0.033	0.034	0.033	0.035	0.035	0.042	0.072	0.131	0.174
51	0.033	0.033	0.033	0.032	0.034	0.032	0.034	0.033	0.034	0.033	0.034	0.034	0.035	0.036	0.037	0.038	0.049	0.096	0.155	0.192
52	0.032	0.031	0.031	0.032	0.031	0.033	0.032	0.033	0.032	0.033	0.033	0.034	0.034	0.035	0.036	0.039	0.057	0.114	0.170	0.203
53	0.029	0.029	0.029	0.028	0.029	0.028	0.028	0.028	0.030	0.029	0.030	0.030	0.032	0.032	0.033	0.037	0.066	0.127	0.176	0.203
54	0.023	0.024	0.024	0.024	0.024	0.024	0.023	0.025	0.023	0.025	0.024	0.026	0.026	0.028	0.028	0.037	0.078	0.139	0.178	0.200
55	0.020	0.020	0.020	0.019	0.020	0.019	0.020	0.020	0.021	0.021	0.023	0.023	0.023	0.023	0.025	0.037	0.088	0.147	0.181	0.198
56	0.019	0.018	0.018	0.017	0.017	0.018	0.018	0.019	0.019	0.019	0.019	0.020	0.020	0.023	0.025	0.039	0.093	0.148	0.179	0.195
57	0.017	0.017	0.017	0.016	0.017	0.016	0.017	0.017	0.019	0.019	0.020	0.019	0.020	0.020	0.024	0.041	0.097	0.148	0.176	0.190
58	0.016	0.016	0.016	0.016	0.016	0.016	0.016	0.016	0.017	0.017	0.019	0.018	0.020	0.021	0.025	0.048	0.107	0.153	0.176	0.189
59	0.015	0.014	0.015	0.015	0.015	0.014	0.014	0.015	0.016	0.016	0.017	0.017	0.019	0.020	0.027	0.065	0.124	0.160	0.178	0.189
60	0.014	0.013	0.013	0.014	0.014	0.014	0.013	0.014	0.014	0.016	0.016	0.016	0.016	0.019	0.029	0.078	0.134	0.164	0.179	0.189
61	0.014	0.013	0.013	0.013	0.013	0.013	0.014	0.013	0.014	0.014	0.015	0.015	0.016	0.018	0.037	0.097	0.148	0.173	0.186	0.194
62	0.013	0.013	0.012	0.014	0.013	0.013	0.013	0.013	0.014	0.015	0.015	0.016	0.017	0.021	0.050	0.114	0.157	0.178	0.192	0.201
63	0.013	0.013	0.013	0.011	0.013	0.011	0.013	0.013	0.014	0.014	0.016	0.016	0.017	0.021	0.062	0.123	0.161	0.180	0.193	0.202

Figure 18. Concluded

TABLES

Table 1. Groove Measurements

0.010-in. Grooves (CONFIG 2)

Groove No. ⟶	1		2		3	
S	W_b	D	W_b	D	W_b	D
0	.009	.055	.008	.060	.006	.070
1/8	.009	.055	.008	.070	.007	.080
1/4	.009	.060	.008	.072	.007	.080
3/8	.010	.060	.009	.065	.008	.085
1/2	.010	.070	.009	.060	.008	.085
5/8	-	.070	.009	.055	.009	.080
3/4	.010	.065	.009	.050	.009	.070
7/8	.010	.060	.009	.050	.009	.065
1	.009	.050	.009	.050	.009	.060
1 1/8	.008	.045	.008	.050	.008	.055
1 1/4	.007	.035	.007	.050	.007	.050
1 3/8	.006	.025	.007	.050	.007	.040
1 1/2			.006	.040	.007	.035
1 5/8			.006	.030	.006	.030
1 3/4					.006	.020
1 7/8						
2						

S - Surface distance along groove, in.

D - Groove depth, in.

W_b - Groove width at bottom of groove, in.

W_s - Groove width at about 0.025-in. below model surface, in.

SEE FIGURE 8c FOR GEOMETRY

Table 1 Concluded

0.030-in. Grooves (CONFIG 3)

Groove No.→	1			2			3		
S	W_b	W_s	D	W_b	W_s	D	W_b	W_s	D
0	.012	.027	.070	.012	.023	.080	.012	.021	.080
1/8	.012	.027	.070	.012	.023	.090	.012	.021	.090
1/4	.014	.027	.070	.012	.024	.100	.012	.022	.100
3/8	.016	.028	.060	.014	.024	.100	.012	.023	.110
1/2	.018	.029	.060	.016	.025	.100	.014	.023	.105
5/8	.018	.030	.070	.018	.027	.100	.014	.022	.100
3/4	.018	.029	.070	.018	.027	.100	.016	.022	.095
7/8	.016	.028	.070	.018	.027	.100	.016	.021	.090
1	.014	.027	.065	.016	.025	.100	.016	.021	.085
1 1/8	.012	.027	.045	.014	.024	.080	.014	.021	.080
1 1/4	.012	.027	.040	.012	.024	.070	.014	.020	.080
1 3/8				.012	.023	.065	.012	.020	.070
1 1/2				.012	.023	.040	.012	.020	.060
1 5/8							.012	.020	.050
1 3/4							.012	.020	.040
1 7/8									
2									

TABLE 2

TEST DATA SUMMARY

a. Blockage Test

Configuration	α, deg	Group Numbers RE/FT x 10^{-6}						
		0.50	1.00	1.25	1.50	2.00	2.50	3.70
0.025-scale	30	3						
	40	1						
	45	2					4	5
0.025-scale with trailing edge extension	40	6,8					17,18	19
	42	10	11				16	20
	43	9						
	45	7		12	13	14	15	

Table 2. Continued

b. 94-0 Models

Configuration	RE/FTx10^{-6}	Group Numbers α,deg	
		30	40
RSI Forward	0.50	39	40
	0.75	37	38
	1.00	13,17,18,21,52	15,16,19,20,35,36
	1.50	32,33,41,44,50	34,42,45,51
	2.00	30,46,47,48	31,49
	2.50	2,3,22,27	4,6,23
	3.00	28,53,54	29,55
	3.50	9,12,24,26	10,11,25
RSI Aft	0.50	96,125,128	97,126,127
	0.75	106,123	107,124
	1.00	88,89,90,104,120,122	91,92,105,121
	1.50	85,86,108,112,118,119	87,109,111
	2.00	93,113,114,117	94,95
	2.50	98,115,116	100,102
	3.00	103	
RCC Novamide	0.50	80	81
	0.75	82	83
	1.00	76,78	77,79
	1.50	60,74,84	61,75
	2.00	58,70	57,59,71
	2.50	62,72,73	63
	3.00	64,69	65
	3.50	67	68

Table 2 Concluded

c. 82-1 and 82-3 Models

Group Numbers

CONFIGURATION	α, deg	CAMERA	$Re_\infty \times 10^{-6}$, ft^{-1} 0.50	0.88	1.60
1 SMOOTH (0.04 FOREBODY-PS)	30	CLOSEUP	250/141, 200/142	250/136, 300/137	350/129, 250/130, 300/132, 250/131
	35		200/143	250/138, 300/139	300/133, 350/134
	40			300/140	300/135
		WHOLE BODY	250/145		
2 ≈0.010" GROOVES	30				250/146
	35				250/147
	40				300/148
3 ≈0.030" GROOVES	30				250/151
	35				250/150
	40				300/149
	30	CLOSEUP			350/152, 450/153, 550/154
	35				550/156
	40				550/155
4 ≈0.030" GROOVES WITH MISSING TILE	30	WHOLE BODY			250/162
	35				250/161
	40				300/160
	30	CLOSEUP			550/157
	35				550/158
	40				550/159

PAINT/GROUP

No valid data for Group 144, tunnel flow breakdown.

TABLE 3

Model Material Thermophysical Properties

94-0 Model

$\sqrt{\rho ck} = 0.0532$ Btu/ft^2-sec$^{1/2}$-$^\circ$R

82-1 and 82-3 Models

T_{pc}, $^\circ$F	$\sqrt{\rho ck}$, Btu/ft^2-sec$^{1/2}$-$^\circ$R
150	0.0505
169	0.0515
175	0.0518
200	0.0529
250	0.0551
275	0.0560
300	0.0568
350	0.0579
400	0.0585
450	0.0581
500	0.0564
550	0.0514

Table 4. Color Interface Temperatures

	Temperature, ^{o}R				
f-stop	1.8			2.5	
sensitivity	200	500	1000	500	1000
Blue-Light Blue	558	600	640	646	694
Light Blue-Green	589	642	692	697	756
Green-Light Green	611	672	728	732	799
Light Green-Violet	629	695	756	760	833
Violet-Magenta	644	715	779	783	861
Magenta-Red	657	732	800	803	885
Red-Orange	668	746	818	821	908
Orange-Yellow	678	760	834	838	928
Yellow-White	689	772	849	852	947

Table 5

Blockage Data Summary

CONFIGURATION	ALPHA-MODEL	RE $x10^{-6}$/FT	BLOCKAGE
0.025 scale	40	0.5	No
	45		
	30		
	45	2.5	
	45	3.8	
0.025 scale w/ T.E.extension	40	0.5	
	45		Yes
	40		No
	43		Yes
	42		Yes
	42	1.0	No
	45	1.25	Yes
		1.5	Yes
		2.0	Yes
		2.5	Yes
	42		No
	40		No
			Yes
		3.8	No
	42	3.8	No